Morphological characterization of aggregates and agglomerates by image analysis: A systematic literature review

Léo Théodon, Johan Debayle, Carole Coufort-Saudejaud

Morphological characterization of aggregates and agglomerates by image analysis: A systematic literature review

L. Théodon[a,*], J. Debayle[a], C. Coufort-Saudejaud[b]

[a] *MINES Saint-Etienne, CNRS, UMR 5307 LGF, Centre SPIN, Saint-Etienne, France.*
[b] *Laboratoire de Génie Chimique, Université de Toulouse, CNRS, INPT, UPS, Toulouse, France.*

Abstract

The morphological characterization of aggregates or agglomerates using image analysis is an increasingly active area of research, whether in the chemical, environmental or civil engineering industries, in the food industry or in the medical and pharmaceutical fields. The final properties of agglomerates are often related to their size and shape distribution, and the morphology of aggregates can in turn influence the efficiency of industrial processes or their impact on health and the environment. Since the morphology of aggregates has such a considerable influence, tools are needed to measure, characterize and quantify it, in particular by image analysis. Therefore, this article proposes to apply the method of Systematic Literature Review (SLR) to answer a series of questions, such as which are the most popular imaging devices, the size and type of aggregates studied, the most active research fields, the most popular image analysis techniques, the most represented authors and journals and, above all, the main morphological characteristics measured, with their definition given in the supplementary material. For this purpose, the SLR method is described in detail, as well as the research questions and the protocol followed. A total of 145 articles were selected based on the inclusion and exclusion criteria, and the data collected are presented. All morphological characteristics measured and reported are presented, described, and defined for a total of more than 45 different morphological characteristics and more than 110 definitions. Techniques for image analysis, aggregate characterization, and the full range of imaging devices used are listed. Finally, other reviews on the study of aggregates or agglomerates are mentioned, and the main points of this article are summarized in a conclusion with some guidelines for future authors.

Keywords: aggregate, agglomerate, morphological characterization, image analysis

1. Introduction

The phenomena of aggregation and agglomeration of objects or particles are at the heart of many fields of research, ranging from biomedicine to civil engineering, including the food and chemical industries. In particular, the morphology of aggregates or agglomerates is usually of critical importance as it has a significant influence on the structural properties of materials and their quality. There are many techniques to characterize the size and morphology of these objects, such as X-ray diffraction (XRD) [1–3], dynamic laser scattering (DLS) [4–6], optical microscopy ([6–10]) or electronic microscopy ([11–14]) to name a few. They provide very accurate data, especially regarding the size of the objects. However, they often require strong assumptions about their shape (sphericity or regularity hypothesis), not to mention other limitations (Fewster [15]). Thus, it is sometimes necessary to directly observe the aggregates or agglomerates to get a more precise idea of their morphology.

For many years, image analysis techniques have been developed to study the morphological properties of aggregates and agglomerates. These techniques can be based on electronic imaging (SEM or TEM), optical imaging, or tomographic imaging, to name a few. Depending on the field of research and the nature of the aggregate, several morphological descriptors are then calculated. The objective of this paper is to propose a literature review of the different techniques of morphological characterization of aggregates and agglomerates by image analysis, in the form of a *Systematic Literature Review* (SLR). It will answer several questions, such as the determination of the most frequently used morphological descriptors to characterize aggregates and agglomerates, the most represented journals and authors among the selected papers, or the most popular imaging devices. As the morphological characterization of aggregates or agglomerates is an extremely broad field, this literature review

*Corresponding author
Email addresses: l.theodon@emse.fr (L. Théodon), debayle@emse.fr (J. Debayle), carole.saudejaud@toulouse-inp.fr (C. Coufort-Saudejaud)

will focus only on articles using experimental data.

The principle of an SLR is to apply the scientific method to a literature review. A set of rules must be defined to minimize bias and subjectivity. The following section describes these principles and defines some research questions and criteria. Then, the main results are presented and the data collected are commented. The next part proposes the creation of an ontology of the morphological characteristics encountered during this literature review. Finally, the imaging devices are presented, as well as different techniques for the characterization of aggregates and agglomerates. The last part proposes a conclusion and a broader view of the subject, with the mention of other literature reviews on the subject of aggregation and agglomeration phenomena. The supplementary material included with this paper contains an exhaustive list of all the definitions of morphological characteristics encountered, as well as the imaging devices used.

2. The principle of an SLR and how to use it

2.1. Definition

A systematic literature review is one of many specific forms of literature review [16] that provide a framework for identifying, evaluating, and interpreting the entire body of existing research in the most accurate and unbiased way possible. The analogy is often drawn to the application of the scientific method to literature reviews. Indeed, anyone applying the same method should get the same results. The idea is to answer a set of questions by following a set of rules. Following the guidelines provided by Kitchenham and Charters [17], we can define six steps (Fig. 1): formulation of the research questions, literature search, initial selection of articles, extraction of data to address the research questions, quality assessment of the selected articles, and data synthesis.

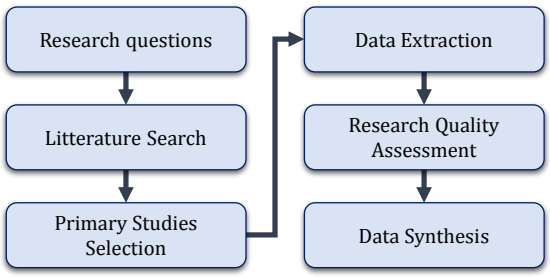

Figure 1: Systematic literature review protocol.

However, although the SLR is theoretically a way to limit bias through the adoption of clear rules and objective selection criteria, the definition of these criteria remains subjective. Thus, one of the complaints that can be raised against this method is the fact that it is possible to miss high quality articles that do not perfectly meet the various selection criteria. In order to overcome this problem, the last part of this paper will propose some references to articles that did not meet the different selection criteria, but are nevertheless of great interest for the study of aggregation or agglomeration phenomena. In the following section, the rules for carrying out a SLR of articles dealing with the morphological characterization of aggregates or agglomerates by image analysis are established.

2.2. Application

2.2.1. Research Questions

The first step in the protocol is to define a set of research questions to be answered by the SLR. Table 1 summarizes these. In particular, there are questions regarding the most important journals and the most influential authors, but also the core of the topic: what are the most commonly used morphological characteristics to characterize the morphology of aggregates or agglomerates by image analysis?

Table 1: Set of research questions formulated in the context of the SLR. All questions are related to the characterization of aggregates or agglomerates by image analysis.

ID	Research Question
RQ1	Which international journals are the most significant?
RQ2	Who are the most significant and influential researchers?
RQ3	What are the most commonly used morphological characteristics?
RQ4	What are the most commonly used image analysis techniques?
RQ5	What type of aggregates or agglomerates are the most studied?
RQ6	What is the average size of the most studied aggregates or agglomerates?
RQ7	What are the most commonly used imaging devices?
RQ8	In which research fields are aggregates or agglomerates most studied?

2.2.2. Literature Search

The article search was performed using Scopus (https://www.scopus.com/) as well as Google Scholar (https://scholar.google.com/). Scopus is a database, mainly of peer-reviewed literature, that includes many publishers and journals with a high impact factor, such as IEEE Journal, ScienceDirect, and Springer. Google Scholar was used to further extend the search to other sources that may not have been referenced in Scopus.

Since the SLR deals with both aggregates and agglomerates (sometimes also called *clumps*, see Nichols et al. [18]), the string used in the literature search is the following:

(Aggregate OR Agglomerate OR Clump) AND (Morphological OR Morphology) AND Image Analysis

Titles, abstracts and keywords were searched. Only conference or journal articles written in English were included. Although very field-specific, the word *Floc* was tried out, but in the end was not used, as it did not increase the number of selected research papers. Finally, only articles published before March 2023 are considered.

A complementary way of searching for research papers when writing a literature review is through reference analysis. This analysis was performed as a preliminary step and showed that

its main effect was to increase the size of the initial list of research papers without significantly increasing the size of the final list of selected research papers. For the sake of simplicity and to make the research paper selectixon protocol more fluid, it was decided to limit the selection process to that described above.

2.2.3. Primary Studies Selection

The selection of papers to be included in the SLR is based on the criteria defined in Table 2. These are journal or conference papers dealing with the morphological characterization of aggregates or agglomerates by image analysis, written in English and supported by experimental data. Review articles or compilations of abstracts are excluded. Fig. 2 illustrates the process of article collection and selection. The initial list obtained from the search string contained 393 articles. An initial selection based on the inclusion and exclusion criteria in Table 2 reduced this number to 221 articles. A final selection based on full text analysis resulted in a final list of 145 articles. This last analysis eliminates articles that have not been peer-reviewed, are not published in international journals, are not considered of sufficient quality, or whose experimental data have not been obtained by image analysis, for example. Criterion C8 is necessary for the sake of clarity, to set a deadline beyond which no more research papers will be considered.

Table 2: List of different selection criteria for the composition of the corpus of articles to be reviewed.

ID	Selection Criteria
C1	Papers with full text available
C2	Papers written in English
C3	Papers published in a scientific journal or conference
C4	Applied research papers (no theoretical articles)
C5	Papers that deal with morphological characterization of aggregates or agglomerates (or clumps)
C6	Morphological characterization with image analysis (at least partly)
C7	No review articles, surveys, or abstract compilations
C8	Papers published before March 2023

2.2.4. Data Extraction

Data extraction is performed on the final list of 145 articles. The data extraction is designed to answer the research questions in Table 1. Table 3 shows some of the data extracted from the articles to answer the research questions. The Sysrev online application (https://sysrev.com/) was used to store the collected data.

2.2.5. Research Quality Assessment and Data Synthesis

The data extraction allows both qualitative and quantitative analysis. The qualitative data include the conclusions of the articles and the quality of the performance of the developed morphological characterization methods by image analysis. These data can sometimes be quite subjective. Quantitative data include the most commonly used morphological characterization and image analysis devices and techniques, as well as the most popular journals or the most represented research fields. These data are more objective because of the SLR framework. In the following, the SLR is presented using the narrative synthesis method. In particular, the following section proposes an overview of the quantitative data collected.

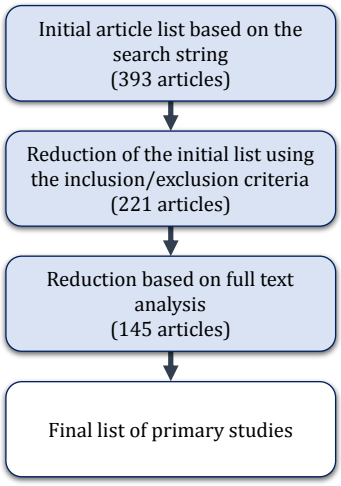

Figure 2: Primary studies selection protocol.

Table 3: Some properties extracted from the articles in order to answer the research questions.

Properties	Research Questions
Researcher and Journal Publication	RQ1, RQ2
Morphological characteristics	RQ3
Image analysis technique	RQ4
Size and type	RQ5, RQ6
Imaging device	RQ7
Research field	RQ8

3. Data analysis

3.1. RQ1 – Journal Publications

In this SLR, 145 articles were analyzed. These 145 articles were published in 101 different journals. The most represented journal is Powder Technology with 21 citations. Fig. 3a shows the journals with at least 3 articles in the final list. Fig. 3b shows the trend of papers proposing to characterize the morphology of aggregates or agglomerates by image analysis. The trend is clearly upward for the last 10-15 years, with the exception of 2023, the current year. It should also be noted that selection criterion C1 specifies that only full-text articles are included, which may explain why some interesting articles are not included in the final list.

3.2. RQ2 – Researchers

Of the 145 selected articles, there are 626 different authors and co-authors. Fig. 4a shows the most represented researchers, with more than 4 publications, and Fig. 4b shows the researchers who published most papers as first author, with at least 2 publications. No particular names stand out among the

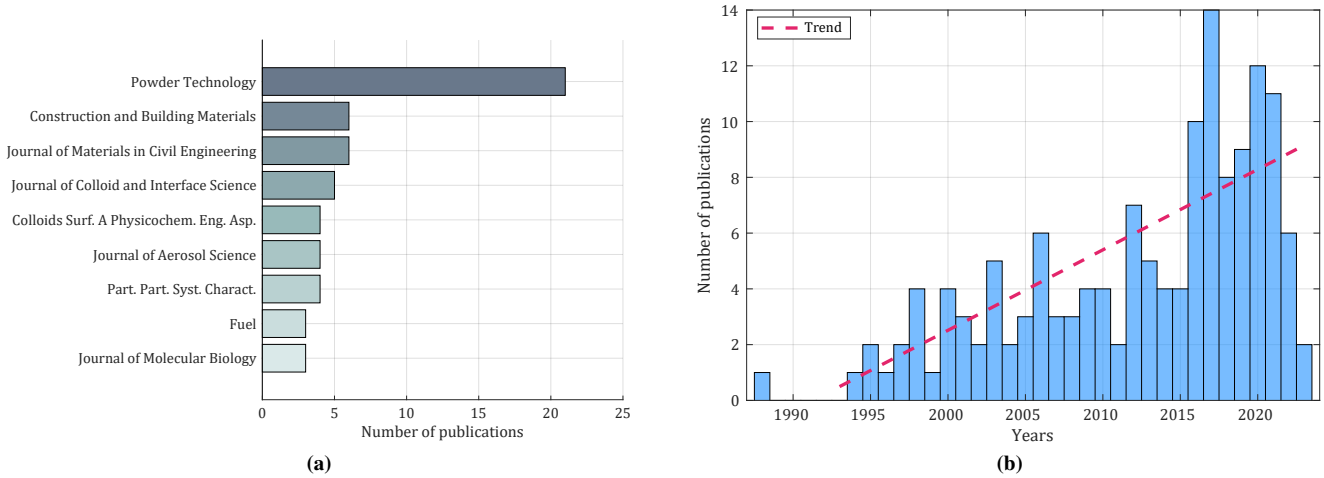

Figure 3: Most represented journals and years of publication with trend line.

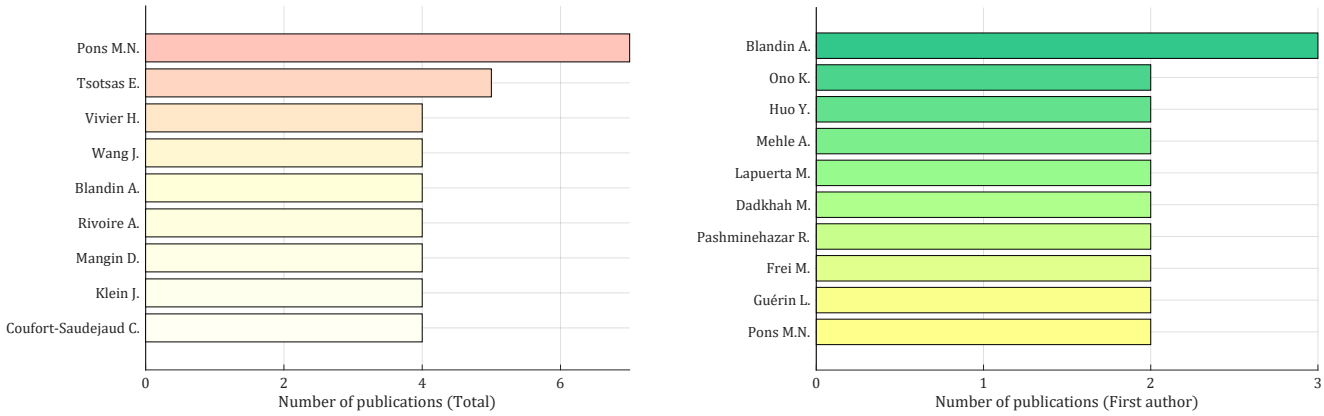

Figure 4: Researchers who published the most papers in total and as first author.

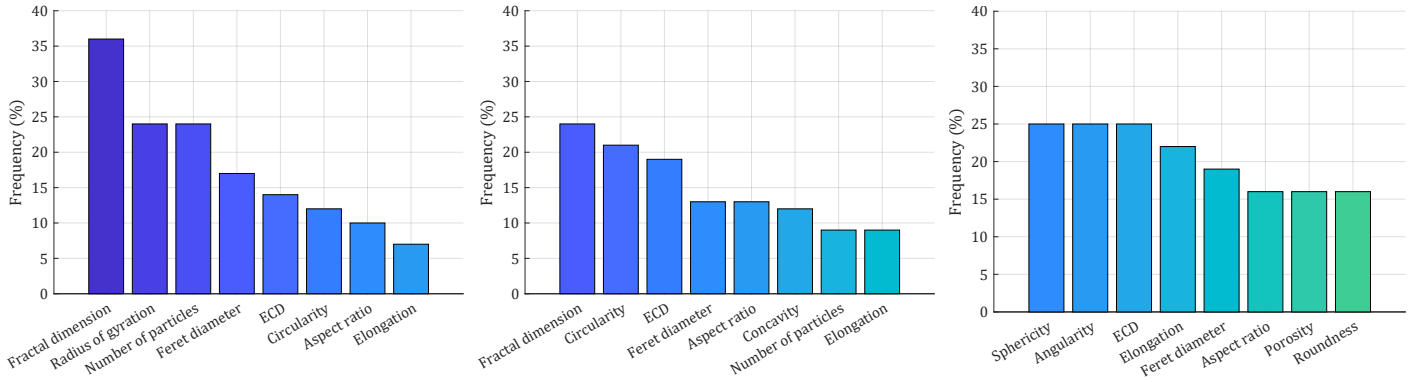

Figure 5: The most common morphological characteristics for aggregates and agglomerates of average size within various ranges.

authors of the selected set of research articles. In fact, although the field of research is extremely broad, the selection criteria are quite restrictive, in particular the need to rely on experimental data. As a result, some highly productive authors in the field of aggregates or agglomerates may not stand out in this literature review. For Fig. 4b, first authors have been preferred to corresponding authors, as is common practice in systematic literature reviews.

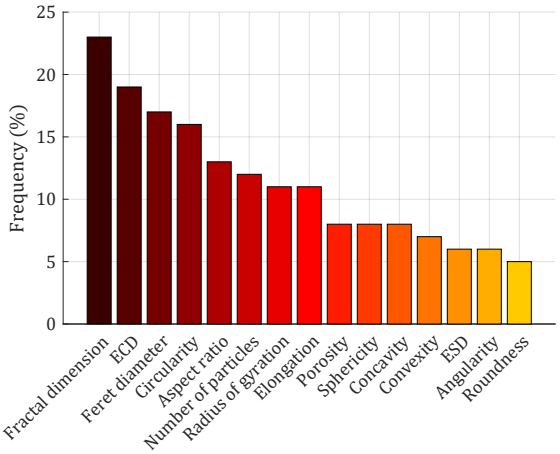

Figure 6: Most common morphological characteristics.

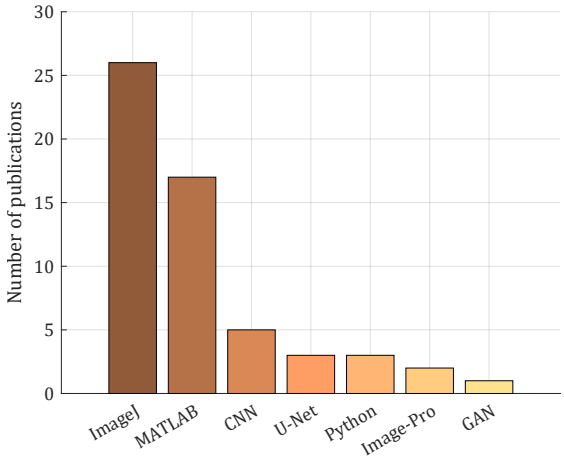

Figure 7: Most common morphological characterization techniques by image analysis.

3.3. RQ3 – Morphological Characteristics

The full-text analysis resulted in the identification of over 50 different morphological characteristics, which are defined in Section 4. Fig. 6 shows the 16 most common morphological characteristics among the 145 articles reviewed. Characteristics such as projected area, perimeter or convex hull are not listed here because they are mostly not used as such to characterize the morphology of aggregates, but allow to define other characteristics such as *circularity*, *sphericity* or *equivalent circle diameter* (ECD). The most represented morphological characteristic is the fractal dimension (23% of the cases), very often calculated for soot particle aggregates, for instance, and often associated with the radius of gyration. Then come two size characteristics: the equivalent circle diameter or ECD (almost 20% of the cases), which is a characteristic calculated independently of the size of the object and used as a size criterion for both the aggregate itself and the primary particles, and the Feret diameter in almost 16% of the cases. Then come some shape characteristics commonly used to characterize the morphology of crystalline agglomerates or coarse aggregates, such as circularity, aspect ratio, or elongation.

Nevertheless, the morphological characteristics measured depend strongly on the size of the aggregates or agglomerates considered. Indeed, Fig. 5 shows which morphological characteristics are most frequently represented for objects of average size within the intervals $[1^{-3}\ \mu\text{m}; 1\ \mu\text{m}[$, $[1\ \mu\text{m}; 10^{3}\ \mu\text{m}[$ and $[10^{3}\ \mu\text{m}; +\infty[$. It is then clear that the fractal dimension and the radius of gyration are the most represented morphological characteristics at small scales (Fig. 5a), as well as the number of primary particles, which is itself a morphological characteristic correlated with the fractal dimension and is often used to characterize the aggregates of soot particles or titanium dioxide, for example. On the other hand, the fractal dimension is no longer one of the most common morphological characteristics at large scales (Fig. 5c), where rocks or coarse aggregates are found. Instead, other shape or texture characteristics, such as angularity or roundness, or other structural characteristics, such as porosity, appear, as well as 3D morphological characteristics, such as sphericity, which can be obtained, for example, from CT scans (X-Ray Computed Tomography). Finally, at intermediate scales (Fig. 5b), most of the morphological characteristics are represented in fairly equal amounts. In fact, many different types of aggregates are present at these scales, with quasi-spherical particle aggregates, where the fractal dimension plays an important role, or crystalline agglomerates, for which the study of morphology will be similar to that of rocks and coarse aggregates.

3.4. RQ4 – Image analysis techniques

Fig. 7 shows which image analysis techniques are most commonly used to characterize the morphology of aggregates or agglomerates. ImageJ is the most commonly used software, mentioned 26 times. The MATLAB® language and its image processing ToolBox are then the most frequently used, far ahead of Python packages such as *scikit-image* (only 3 references). Other techniques are mentioned, including the use of machine learning techniques, usually coded in Python, with custom Convolutional Neural Networks (CNN), U-Net networks, Generative Adversarial Networks (GAN), and finally a competitor of ImageJ: Image-Pro. It should be noted, however, that only 40% of the 145 articles explicitly state how the images were analyzed, so the information collected is not complete.

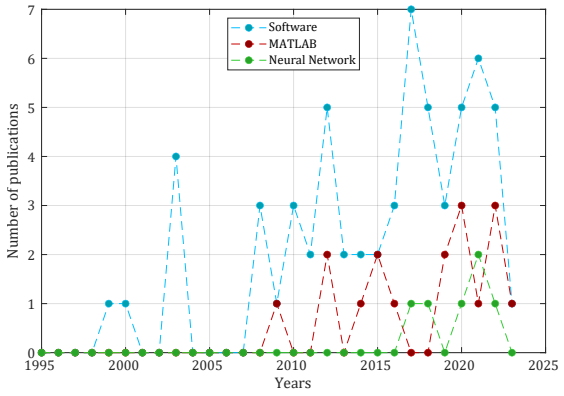

Figure 8: Number of publications per year for various image analysis techniques.

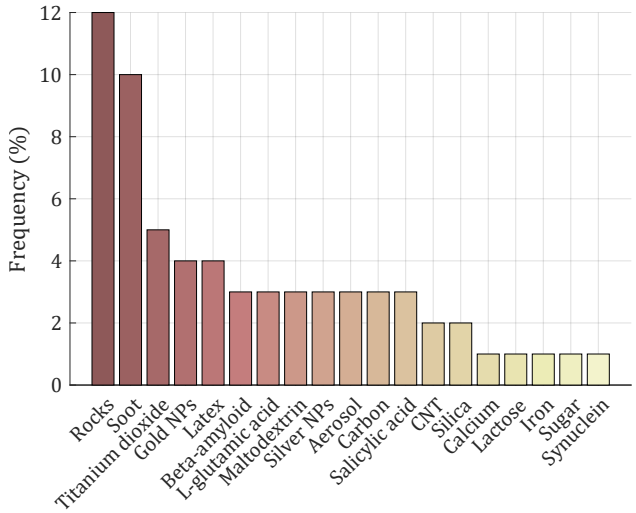

Figure 9: Type of aggregates or agglomerates most studied by image analysis.

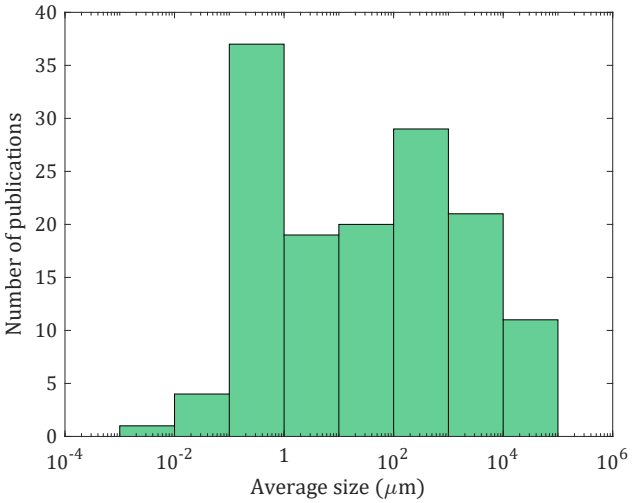

Figure 10: Average size of aggregates or agglomerates studied among the selected research papers.

Fig. 8 shows the evolution over time of the number of publications claiming to use a software (ImageJ or Image-Pro), the MATLAB language, or machine learning techniques. All three trends are clearly increasing, with a very recent start for machine learning techniques (average year of publications using machine learning: 2020).

3.5. RQ5 – Type of aggregate or agglomerate

The fifth research question concerns the most commonly studied type of aggregate and agglomerate (Fig. 9). The most common aggregates are grouped under the term *rock*, with a frequency of occurrence of about 12%. These are the rock aggregates or coarse aggregates found in asphalt mixtures, cement and concrete, and are particularly studied in the field of civil engineering because of the influence of the morphology of the aggregates on the physical properties of the materials [19–36].

In the second place there are aggregates of *soot* type, which are especially studied in environmental engineering, because of their very significant impact on the environment and health. The morphology of these aggregates has an impact on their optical properties [37], and ultimately on global warming [38–42]. It also affects the ability of these aggregates to cause lung disease [42–49].

Many articles (about 5%) also focus on the case of titanium dioxide. These aggregates are widely used in the food [50] and pharmaceutical industries [51], and their morphology can have a significant influence on their toxicity [52, 53]. Gold nanoparticle aggregates are also being investigated, not only because of their potential toxicity [54] or their use in forensic science [55], but also because their morphology has a strong potential for surface-enhanced Raman scattering [56–58].

Latex nanoparticle aggregates are also strongly represented (about 4%), either as part of the study of the aggregation process itself [59, 60], or because of the influence of the aggregate morphology on the quality and physical properties of the powder obtained at the end of the process [6, 8, 61, 62]. The study of latex aggregates is very important because they can be used as *model* particles, just like maltodextrin aggregates [63–66], to test experimental devices, new characterization techniques or models.

Protein aggregates such as amyloid have been extensively studied by atomic force microscopy (AFM) because their morphology has a strong influence on the risk of neurodegenerative diseases [67], such as Parkinson's [68, 69], Alzheimer's [70, 71], Creutzfeldt-Jakob [72] or Huntington's [73].

In total, nearly 50 types of aggregates or agglomerates are represented within the corpus of 145 selected articles, but slightly more than 60% of the articles focus on less than 20 different types of aggregates or agglomerates.

3.6. RQ6 – Average size

For each of the selected articles, the average size of the aggregates or agglomerates studied was determined from the data provided. The results are shown in Fig. 10. The interval [100 nm; 100 μm] corresponds to more than 50% of the articles, and the interval [100 nm; 1 mm] to almost 75% of the articles.

Overall, the size of the studied objects varies widely, from a few nanometers for the smallest (gold nanoparticles, Dai et al. [55]) to several centimeters for the largest (coarse aggregates, Kuo et al. [20]).

3.7. RQ7 – Imaging device

The seventh research question concerns the most common devices used to capture images of aggregates or agglomerates. These may be optical devices such as optical microscopes (OM), high-resolution or high-speed cameras (hereafter referred to as *cameras*), or the use of multiple cameras. Other techniques include scanning electron microscopy (SEM), transmission electron microscopy (TEM), atomic force microscopy (AFM), and X-ray computed tomography (CT scan). Fig. 11 shows the most commonly used imaging devices, with some articles using more than one.

Electron microscopy technologies such as SEM and TEM are clearly the most represented. Optical microscopy appears in

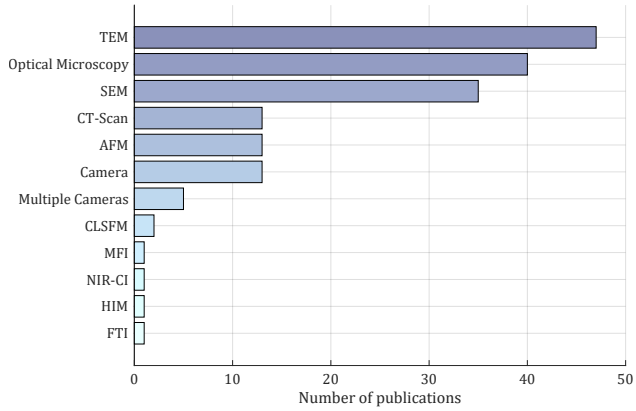

Figure 11: The most commonly used equipment for capturing images of aggregates or agglomerates.

just over 25% of the publications studied, and the use of cameras (single or multiple) accounts for only 18% of the publications. Cameras as such are mainly used for the characterization of rocks or coarse aggregates. In such cases, CT scanning is sometimes also used to determine the internal structure and quality of the material [24, 26, 28]. Confocal laser scanning fluorescence microscopy (CLSFM) is used in two papers to obtain better contrasts [74] and to detect aggregates at very low concentrations [61]. Other techniques are discussed in more detail in the following sections.

3.8. RQ8 – Research fields

Fig. 12 shows the most common research fields in the corpus of selected research papers, noting that a single paper may belong to more than one research field. For example, the field *Chemical Engineering* is the most common. A certain balance is maintained among the research fields, ranging from chemical engineering to environmental engineering, and from materials science and civil engineering to medicine and pharmaceuticals.

Just over 10 publications focus primarily on image analysis techniques for the morphological characterization of aggregates or agglomerates and therefore belong to the research area entitled *Image Analysis* [62, 75–85].

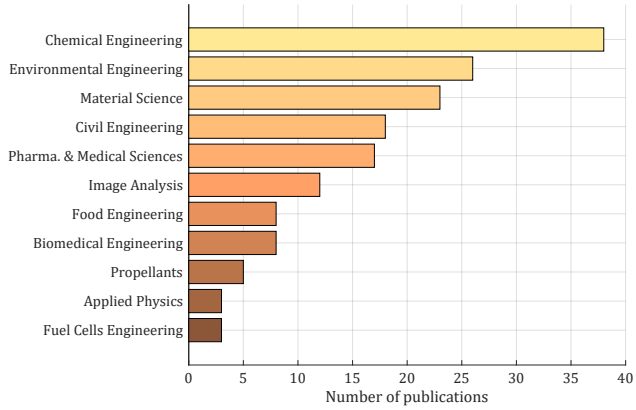

Figure 12: The most active research areas in the morphological characterization of aggregates or agglomerates using image analysis.

In the field of food engineering, the morphological characterization of aggregates is useful for controlling the visual appearance [64, 86] and taste of products [65, 66], as well as their solubility [87–89], especially in the case of food powders.

Biomedical engineering is represented with almost 10 papers on fiber-like protein aggregates, whose morphology is responsible for many neurodegenerative diseases [67–73, 90].

In the field of propellant research (5 papers selected), the morphology of aggregates can have an impact on both health and the environment, as in the case of biodiesel fuels [91], but also on performance [92, 93], as in the case of rocket propellants [94, 95].

Three articles have been categorized as *Applied Physics* because they deal with topics such as the calculation of the breakup energy of the agglomerate [96], the influence of the morphology of an aggregate of superparamagnetic particles on its behavior in an anisotropic liquid [97], or the phenomena of nonlinear agglomeration of colloids under microgravity [98].

Finally, three articles fall within the research field of fuel cell engineering, where the morphology of aggregates within the microstructure of fuel cells has an impact on the performance [99–101].

4. Morphological characteristics

This section lists the morphological characteristics used by the selected research articles. These morphological characteristics can be divided into five main categories: *size*, *shape*, *angularity*, *texture*, and *structure*. Fig. 13 is an attempt to illustrate the differences between four of these categories.

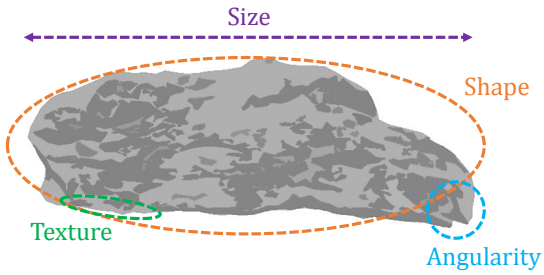

Figure 13: Morphological characterization of an aggregate: size, shape, angularity and texture.

Clearly, while this classification makes sense for rocks and coarse aggregates, it is much less relevant for characterizing aggregates that resemble clusters of spherical nanoparticles, such as titanium dioxide aggregates. Nevertheless, it can be observed that as the size of the aggregate decreases, certain categories are used less frequently, starting with texture descriptors and then angularity. They are usually simply omitted and very often, when the average size of the aggregate drops to less than a micrometer, the radius of gyration acts as the only size characteristic and the fractal dimension as the only shape characteristic, as shown in Fig. 5 – which shows the most frequently used morphological characteristics with respect to the average size of the

Size Characteristics

Characteristic	Symbol	Nb. of definitions	Nb. of occurrences	Size repartition (μm)
Projected Area	A_p	1	63	
Perimeter	P	1	31	
Equivalent Circle Diameter	ECD	1	27	
Feret Diameter	F	1	23	
Length	L	5	18	
Number of Primary Particles	N_p	1	17	
Radius of Gyration	R_g	4	16	
Diameter	d	2	9	
Height	H	1	8	
Equivalent Spherical Diameter	ESD	1	8	
Surface Area	S	1	5	
Width	W	2	4	

Table 4: List of the 12 size characteristics, along with their associated symbol, the number of occurrences in the set of selected research papers, the number of different definitions, and the distribution of the average size of the aggregates or agglomerates on which they are measured. The red marker on the box plots represents the median.

aggregates studied – and Tables 4 and 5 – which list the size and shape characteristics mentioned in the 145 articles studied.

In order not to overload the present article with the many different definitions of each of the morphological characteristics, the reader can find more detailed information in the supplementary material attached to this paper, which contains all the definitions for each of the characteristics, the size of the objects studied and their nature, as well as the corresponding bibliographical references.

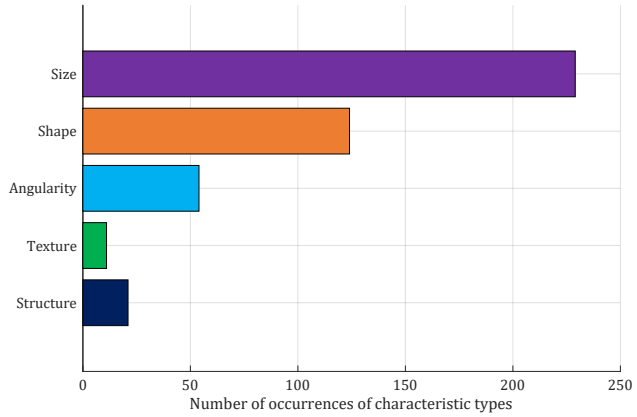

Figure 14: Average size of aggregates or agglomerates studied among the selected research papers.

Fig. 14 shows the number of occurrences of each type of characteristic mentioned in the 145 research articles. On average, there were just over 3 characteristics per article. Size characteristics are the most frequently measured, not only because they are significant on their own, but also because they can be used to define other types of characteristics, such as shape and angularity. However, image analysis measurements are sensitive to resolution and noise, making it more difficult to make certain measurements robust. Fig. 14 illustrates a correlation between the number of occurrences of characteristic types and the difficulty of measuring them. In fact, it's easier to measure the overall size of an object than to assess its angularity or qualify the texture of its contour. In fact, by analyzing Tables 6 and 7, it can be seen that the measurement of angularity and texture characteristics mainly concerns aggregates and agglomerates whose size exceeds several hundred micrometers or even a few tens of millimeters. This can be explained not only by the nature of the objects studied, but also by the precision of the imaging devices used to obtain an image of sufficient quality to make such measurements.

4.1. Size characteristics

Size characteristics are of particular interest when characterizing an object. Not only do they provide information about the actual size of the object (length, diameter, area, volume) or its contour (perimeter, surface area), but they can also be used to define shape characteristics (circularity, elongation) or angularity characteristics (convexity, concavity).

Table 4 lists all 12 size characteristics identified in the 145 selected research articles, sorted in descending order by number of occurrences. The two most frequently measured size characteristics are projected area and perimeter, which makes sense because although the raw value of these characteristics is generally not used as such to characterize the size of an aggregate or agglomerate, they do allow other size characteristics to be defined, such as equivalent circle diameter (ECD) or radius of gyration (R_g) according to certain definitions.

In particular, 73 out of 145 articles (just over 50%) propose PSD (particle size distribution), where the size characteristic is

Shape Characteristics

Characteristic	Symbol	Nb. of definitions	Nb. of occurrences	Size repartition (μm)
Fractal Dimension	D_f	7	33	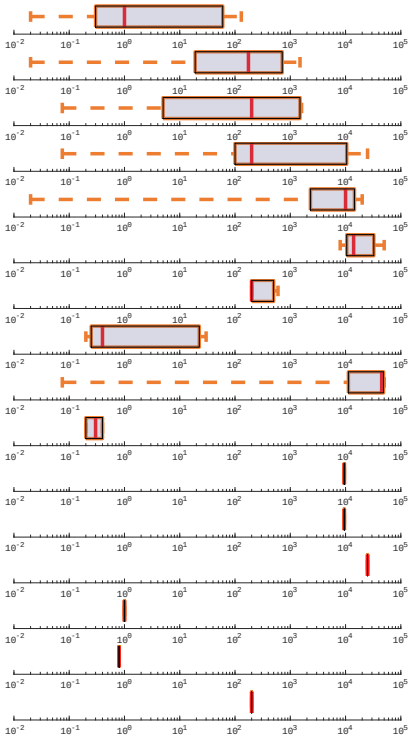
Circularity	C	5	26	
Aspect Ratio	AR	7	17	
Elongation	E	8	15	
Sphericity	Φ_S	10	12	
Flatness	f_{flat}	2	4	
Compactness	O	2	3	
Anisotropy	X	1	3	
Shape Factor	SF	2	3	
Complexity	Y	1	2	
Section Aspect Ratio	SAR	1	1	
Plane Geometry Factor	PGF	1	1	
Axial Coefficient	–	1	1	
Eccentricity	Ec	1	1	
Fractal Area	A_F	1	1	
Robustness	Ω_1	1	1	

Table 5: List of the 16 shape characteristics, along with their associated symbol, the number of occurrences in the set of selected research papers, the number of different definitions, and the distribution of the average size of the aggregates or agglomerates on which they are measured.

usually either the equivalent circle diameter, the Feret diameter, the length or the radius of gyration. Table 4 confirms that the radius of gyration is the most popular criterion for "small" aggregates (below a micrometer), while the Feret diameter is widely used for "large" aggregates (above 100 micrometers), and the ECD is used fairly consistently at virtually all scales, and is generally replaced by the equivalent spherical diameter (ESD) when objects are "larger" (above a millimeter) and it is possible to obtain 3D information, usually using a multi-view imaging device.

4.2. Shape characteristics

Shape characteristics are the most diverse and show the greatest disparity according to the size of the objects studied. In fact, Table 5 lists all 16 shape characteristics mentioned by the 145 selected research articles, and it is clear that the fractal dimension is not only the most frequently measured characteristic (33 occurrences), but also virtually the only characteristic used to characterize the shape of sub-micron objects. For medium-sized objects (from a few tens to a few hundred microns), circularity and aspect ratio are the most common, although there are no less than 15 different definitions for these two quantities. Finally, for larger objects, elongation is favored, again with a large number of different definitions, with sphericity taking over at larger scales (above 10 millimeters) where 3D information can be recovered.

A notable difference that is not visible in Table 5 regarding the use of one property over another, beyond the size of the measured object, is the nature of the latter, and a fortiori the scientific field or community involved in the corresponding article. For example, strain is widely used to characterize large objects such as rocks and coarse aggregates [23, 34–36]. Nevertheless, several definitions of elongation (out of a total of 8) are used to talk about the ratio aspect (7 different definitions) in the characterization of smaller aggregates (silver [102] and silica [103] nanoparticles, lactose crystals [104] , ...), studied by other communities.

In addition, shape characteristics are particularly studied, as they have at least as great an impact as size characteristics on the physicochemical or mechanical properties of the studied objects, such as their toxicity [12, 50, 51], taste [7, 66], environmental impact [39, 40, 43, 44, 48], mechanical strength [24, 25, 105], etc.

4.3. Angularity characteristics

Angularity characteristics are used to quantify the asperities present on the contour of an object more precisely than shape characteristics, which are more general in nature but do not deal with the micro-variations reserved for texture characteristics. Table 6 lists all the angularity characteristics mentioned in the 145 research articles.

While shape characteristics are generally fast and easy to evaluate (e.g., as a ratio of size characteristics), and therefore particularly well suited for real-time applications, angularity characteristics can be computationally intensive, sometimes requiring analysis of the entire contour of an object, with possible

Angularity Characteristics

Characteristic	Symbol	Nb. of definitions	Nb. of occurrences	Size repartition (μm)
Concavity	CAV	6	14	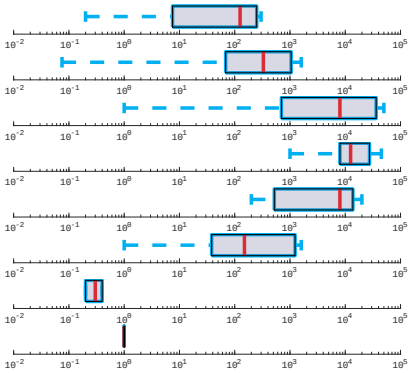
Convexity	CO	4	9	
Roughness	RO	4	8	
Angularity	AF/AI	6	8	
Roundness	R	4	7	
Solidity	SLD	2	5	
Coverage Ratio	Z	1	2	
Extent	–	1	1	

Table 6: List of the 8 angularity characteristics, along with their associated symbol, the number of occurrences in the set of selected research papers, the number of different definitions, and the distribution of the average size of the aggregates or agglomerates on which they are measured.

Texture Characteristics

Characteristic	Symbol	Nb. of definitions	Nb. of occurrences	Size repartition (μm)
Texture	TX/TF	3	6	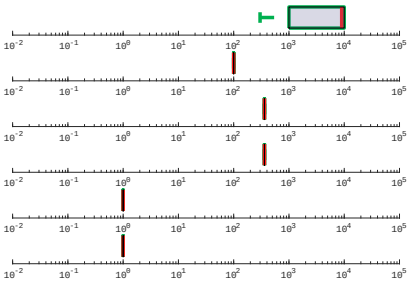
Simplicity	Si	1	1	
Heterogeneity	–	1	1	
Clumpiness	–	1	1	
Lacunarity	Λ	1	1	
Signature	–	1	1	

Table 7: List of the 6 texture characteristics, along with their associated symbol, number of occurrences in the set of selected research papers, number of different definitions and distribution of the average size of the aggregates or agglomerates on which they are measured.

Structure Characteristics

Characteristic	Symbol	Nb. of definitions	Nb. of occurrences	Size repartition (μm)
Porosity	ε	5	11	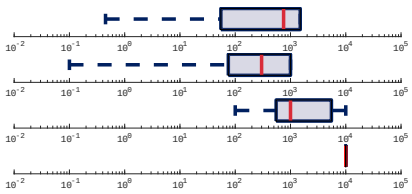
Agglomeration Degree	AD	3	5	
Coordination Number	–	1	4	
Packing Density	η	1	1	

Table 8: List of the 4 structure characteristics, along with their associated symbol, the number of occurrences in the set of selected research papers, the number of different definitions, and the distribution of the average size of the aggregates or agglomerates on which they are measured.

resolution of small optimization problems. On the other hand, they provide a more precise understanding of the morphology of the object under study.

4.4. Texture characteristics

Texture characteristics are mainly used for very fine contour characterization of the "largest" objects (a few hundred microns to a few millimeters minimum), as shown in the table 7. In particular, many texture characteristics (texture factor – TF, texture index – TX) are based on a combination of Fourier descriptors [23, 36, 81] or a wavelet transform [22, 25]. Most of the texture characteristics are used for rocks and coarse aggregates, as well as some crystalline aggregates.

4.5. Structure characteristics

In terms of structure characteristics, porosity accounts for over 50% of the measurements of this type within the 145 articles selected. Measurements of porosity, coordination number, or packing density are performed on rather "large" objects (several hundred micrometers to several millimeters) as shown in Table 8 and require special imaging techniques to probe the internal structure of the objects, such as computed tomography (CT).

Because of the difficulty of implementation, structure characteristics, as well as texture characteristics, are the least used, even though they provide invaluable data.

Imaging device	Nb. of occurrences	Size repartition (μm)
Electronic Microscopy	**82**	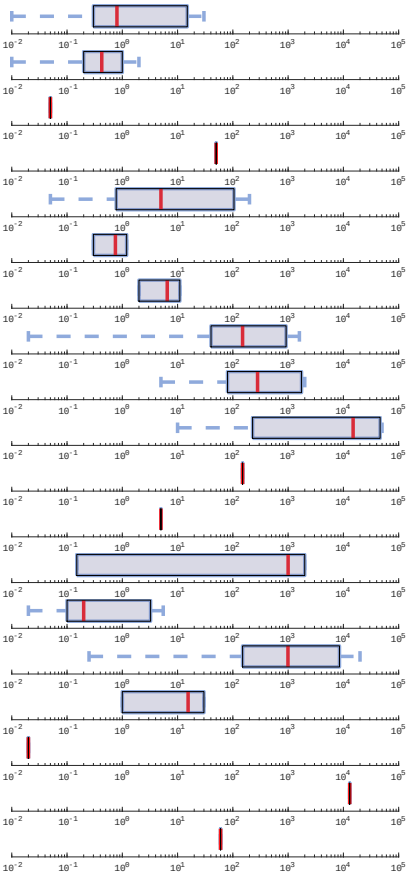
TEM	47	
HR-TEM	1	
Cryo-TEM	1	
SEM	35	
FE-SEM	2	
ESEM: Wet-SEM	2	
Optical Microscopy	**40**	
High Speed Camera	5	
Multiple Cameras	4	
Stereomicroscopy	1	
Shadowgraph Imaging	1	
Particle Tracking Analysis	2	
Atomic Force Microscopy	**13**	
Tomography	**13**	
Laser Confocal Fluorescence Microscopy (LCFM)	**2**	
Helium Ion Microscopy	**1**	
Fourier Transform Interferometry	**1**	
Digital Inline Holography	**1**	

Table 9: List of imaging devices used by the 145 selected research papers.

5. Imaging Devices

A variety of imaging devices are used to capture and produce the images examined in all of the selected research articles. A brief overview of these different imaging devices and the average size range of the objects for which they are used is provided in Table 9. For more information on the scientific context in which these imaging devices are used, as well as the size and nature of the objects studied, readers are invited to consult the supplementary materials that accompany this paper.

In general, it can be observed that electronic imaging techniques are used for the smallest objects (less than 100 micrometers), with transmission electron microscopy being widely used for small aggregates such as soot [39, 40, 46, 49] and aerosol particle aggregates [75, 106, 107] as well as nanoparticle aggregates such as silver [102, 108], gold [55, 109, 110] or titanium [50, 52, 85], and the scanning electron microscope for slightly larger objects, such as crystalline aggregates [77, 79, 111, 112]. At smaller scales, atomic force microscopy is also well represented and is particularly used in the biomedical field, especially for its ability to provide data in a non-destructive way [68–70, 72, 73, 90].

Optical microscopy, on the other hand, is mainly used for objects from a few tens of microns to a few centimeters in size. In particular, it offers great flexibility of use over a very wide range of size scales and has the advantage of being relatively easy to set up compared to electron microscopy techniques. Finally, tomography techniques are mainly used to probe the structure of ”large” objects, i.e. from a few hundred micrometers to tens of millimeters.

6. Image Analysis Techniques & Characterization

Among the selected research articles, numerous techniques and indicators are proposed to measure and/or quantify the way elementary particles agglomerate, to classify aggregates within a population, or simply to calculate the various morphological characteristics of aggregates or agglomerates. This section gives a brief overview of the different techniques used to characterize the morphology of aggregates through their morphological properties. In general, optical and/or electronic imaging devices account for the vast majority of cases (over 90%), while others, such as X-ray tomography, represent only a tiny minority of cases, due to their cost, but also to the difficulty of setting them up and the fact that they are not always suitable.

6.1. Image Analysis and Pattern Recognition

The measurement of morphological features by image analysis sometimes requires the development of new techniques.

Deep-Learning & Machine-Learning

Reference	Year	Model	Accuracy	Avg. size (μm)	Type	Imaging Device	Research Field
Frei and Kruis [83]	2020	Mask R-CNN	0.96	–	Nano-material powders	SEM	Image Analysis
Frei and Kruis [82]	2018	ANN	0.62	–	–	TEM, Simulation	Image Analysis
Monchot et al. [84]	2021	Mask R-CNN	0.95	5.10^{-1}	Titanium dioxide	SEM	Image Analysis
Rühle et al. [85]	2021	GAN & U-Net	0.73 – 0.90	2	Titanium dioxide	TEM, SEM	Image Analysis, Material Engineering
Lins et al. [113]	2022	Mask R-CNN	0.84	10^2	L-alanine crystals	Optical microscope	Chemical Engineering
Mehle et al. [7]	2017	DBSCAN & CNN	0.93	10^3	Pharmaceutical pellets	Optical microscope	Pharmaceutical and Medical Engineering

Table 10: List of papers using deep-earning or machine-learning techniques for pattern recognition and classification.

This section gives a brief overview of the most original and/or widely used methods.

6.1.1. Image Segmentation

One of the most important steps in image analysis is the segmentation or binarization of images to isolate regions of interest, which can then be measured and characterized. In the vast majority of cases (as in Tohno and Takahashi [75]), segmentation is performed by global thresholding based on the Otsu method [114]. However, a global threshold does not capture all the subtleties of certain contours, nor the slight differences in brightness that may exist within an image. For this reason, local thresholding is generally preferable, with the drawbacks of increased computation time and the importance of the parameters to be adjusted [115]. For example, to segment images of coke aggregates, Ershov et al. [80] proposes a local and adaptive segmentation method based on dividing the image according to a grid of variable size. Another method proposed by Pons et al. [78], which does not require the definition of a local or global threshold, is the watershed segmentation, which allows the detection of contact points between different objects. Finally, since the ImageJ software allows the use of local and global thresholds, as do Matlab and most Python libraries, it may be advisable to always test the use of a local threshold before choosing the Otsu method.

6.1.2. Sparse Hough Transform

To obtain the size distribution of aerosol particle aggregates, Einar Kruis et al. [106] proposes the use of the Sparse Hough Transform, which is very effective when the particles to be detected are quasi-spherical, as is often the case at the nanometer scale. Although this circle detection technique is quite old, it is still widely used, including by software such as ImageJ.

6.1.3. Deep Learning & Machine Learning

With the ever-increasing computing power of computers, more and more papers are proposing the use of not only machine learning techniques for object classification, but also deep learning techniques for image processing and pattern recognition, as shown in Table 10.

These methods are almost exclusively based on convolutional neural networks (CNN), with the Mask R-CNN architecture being by far the most popular (Frei and Kruis [83], Monchot et al. [84], Lins et al. [113]). It is a particularly effective model for instance-based object detection and segmentation. Other popular class-based (or semantic) segmentation models based on U-Net are also studied (Rühle et al. [85]), as their effectiveness and robustness in detecting contours and texture differences is well established (Bals and Epple [116]). These are compared in the same article with models based on GANs (Generative Adversarial Network), and are shown to perform slightly better.

For its part, Mehle et al. [7] proposes a workflow in which the areas of interest in an image are determined using the DBSCAN algorithm (Ester et al. [117]). A convolutional neural network (CNN) is then trained to detect primary particles and classify pharmaceutical pellet aggregates by size and morphology.

Image analysis and classification techniques based on machine learning and/or deep learning have many applications in the medical, pharmaceutical, and food industries, where quality control, non-invasive and non-destructive techniques, and real-time applications are particularly sought after.

6.2. Classification

Object classification is a particularly fertile field, and with the advent of machine learning and deep learning in recent years, a wide range of techniques are available. Since image analysis allows the determination of numerous numerical values by calculating morphological features, Principal Component Analysis (PCA) is a technique that is particularly and very often used in the literature to classify aggregates or agglomerates within a heterogeneous population.

6.2.1. Principal Component Analysis (PCA)

For example, Ålander et al. [11] applies PCA to a set of morphological descriptors of paracetamol crystal agglomerates to classify the samples according to the different solvents used, and concludes that only two descriptors (one 2D and one 3D) are needed to distinguish them accurately. Meanwhile, Huo et al. [118] uses PCA to control the process of KDP crystal agglomeration from two consecutive images, combined with the approximate nearest neighbor search algorithm to match the results obtained from one image to the next. Finally, De Temmerman et al. [103] uses PCA to reduce 23 morphological features to a set of three classes (size, shape, and surface topology) to differentiate amorphous silica aggregates according to their production process. Unlike all machine learning techniques, PCA has the advantage of not requiring a learning process. On the other hand, it can sometimes be too slow to be used directly in real-time applications.

6.2.2. Discriminant Factorial Analysis (DFA)

Faria et al. [86] combines image analysis and discriminant factorial analysis (DFA) techniques to automatically classify

sucrose crystal agglomerates according to their shape and other morphological characteristics, such as their degree of agglomeration. The results obtained are quite good, with an agreement of about 90% between automatically and manually classified data. This technique does not require a learning phase and can be easily adapted to quality control in the food and pharmaceutical industries.

6.2.3. Neural Network

Neural networks have been used for many years to classify aggregates or agglomerates based on their morphological characteristics (Ros et al. [119]). Bernard-Michel et al. [76] uses a neural network to classify potassium chloride crystals according to their morphology, using Fourier descriptors and morphological concavity descriptors as the main features. In particular, the classification distinguishes crystals of different shapes as well as crystal agglomerates. For its part, Frei and Kruis [82] proposes to train neural networks to classify TEM images according to the morphology of particle aggregates with different PSD (particle size distribution), transmission coefficients or deformations, with rather promising results.

6.2.4. Support Vector Machine (SVM)

Ochsenbein et al. [120] proposes to use classification techniques based on morphological characteristics of L-glutamic acid crystal aggregates to detect them and to measure the agglomeration process automatically. The implemented classification is based on the machine learning technique called Support Vector Machine (SVM) and allows to characterize the agglomerates by estimating their volume. The method seems to be particularly effective due to the non-linear nature of the data separation possible with an SVM.

Huo et al. [121] uses spectral regression kernel discriminant analysis (SRKDA), linear minimum distance classification (LMDS) and a PCA to define a classification model for agglomerates of L-glutamic acid crystals. Numerous morphological features and Fourier descriptors are computed and PCA is applied to reduce the dimensionality of the problem. The model used to classify the agglomerates according to their shape is an SVM, with a 96% accuracy rate for agglomerate recognition, which is in the high average range, and a processing time of about 8 s on a personal machine, which is relatively fast.

6.2.5. Decision Tree

Fernandez Martinez et al. [81] proposes an original method to classify carbon black nanoparticle aggregates by image analysis, based on their morphological characteristics. Many size and shape characteristics are measured, as well as Fourier descriptors. A PCA is performed to reduce the dimensionality of the problem, and the aggregates are then classified using decision trees based on evolutionary algorithms. The accuracy of the results is on the order of 75%, which is quite good for automatic classification.

In the very specific case of *carbon black* nanoparticle aggregates, ASTM standard D3849-07 identifies a number of characteristics that have a significant effect on the physical properties of the aggregates. Carbon black nanoparticle aggregates are then generally classified into four different groups according to their morphology (spheroidal, ellipsoidal, linear and branched). Fernandez Martinez et al. [81] also adopts this classification from López-de Uralde et al. [122], which proposes an automatic machine learning categorization of carbon black nanoparticle aggregates with an accuracy ranging from 49% to 84%.

6.3. Agglomeration Characterization & Measurement

6.3.1. Complex Network

Machado et al. [54] proposes a complex network approach to analyze the agglomeration process of gold nanoparticle aggregates. Complex networks are represented by graphs, where each vertex is a primary particle and two vertices are connected if they are part of the same aggregate. The structure of the aggregates is thus closely related to the topology of the graphs, and numerous indicators of structure are defined, such as the silhouette, which is calculated as a function of the number of adjacent vertices, and the distance to neighboring graphs. A measure of the internal cohesion of the aggregates and their separation in space is thus defined. The method is robust to large numbers of primary particles, a common limitation of more conventional methods.

6.3.2. Agglomeration Index

Although theoretical and not part of the selected set of research articles, Matsutani and Shimosako [135] proposes a new geometric index called γ_{agg}, related to the Euler number and obtained by image analysis, to estimate the degree of agglomeration of a set of primary particles. The advantage of this method is that it can be carried out entirely by global measurements obtained by image analysis and does not require the determination of particle centers, as is the case for the Clark-Evans index (Petrere [136]), which is also associated with the degree of agglomeration.

6.4. 3D Modeling

Sometimes the use of a model allows us to gain a better understanding of the geometry and morphology of the objects under study. For example, the use of a model can provide more information about the internal structure of aggregates, or allow 3D properties to be predicted from knowledge of 2D properties.

6.4.1. Stochastic Modeling

The use of a stochastic geometric model can be used to predict the 3D properties of an aggregate from 2D properties measured on projected images. Theodon et al. [62] suggests a parametric geometric model for compact aggregates. The model parameters are adjusted to match the 2D properties to those measured on projected images of latex nanoparticle aggregates. The 3D properties such as volume, surface area, and equivalent sphere diameter (ESD) are then obtained with an error on the order of 5%.

Stochastic modeling is also popular when dealing with the porosity and internal structure of aggregates, as in [3] for mesoporous alumina microstructure or [137] which attempts to simulate spray fluidized bed agglomeration.

Review list

Year	Reference	Title
2002	Nichols et al. [18]	A Review of the Terms Agglomerate and Aggregate with a Recommendation for Nomenclature Used in Powder and Particle Characterization
2004	Lee and Kramer [123]	Prediction of three-dimensional fractal dimensions using the two-dimensional properties of fractal aggregates
2009	Philo [124]	A critical review of methods for size characterization of non-particulate protein aggregates
2011	Sorensen [125]	The Mobility of Fractal Aggregates: A Review
2013	Komba et al. [126]	Analytical and Laser Scanning Techniques to Determine Shape Properties of Aggregates
2014	Amin et al. [127]	Protein aggregation, particle formation, characterization & rheology
2018	Jeldres et al. [128]	Population balance modeling to describe the particle aggregation process: A review
2019	Ruggeri et al. [129]	Atomic force microscopy for single molecule characterization of protein aggregation
2019	Zhang et al. [130]	Evaluation methods and indexes of morphological characteristics of coarse aggregates for road materials: A comprehensive review
2020	Thaker and Arora [131]	Measurement of aggregate size and shape using image analysis
2020	Lotito and Zambelli [132]	Pattern detection in colloidal assembly: A mosaic of analysis techniques
2020	Watanabe-Nakayama et al. [133]	High-Speed Atomic Force Microscopy Reveals the Structural Dynamics of the Amyloid-β and Amylin Aggregation Pathways
2021	Gong et al. [134]	Characterization and evaluation of morphological features for aggregate in asphalt mixture: A review

Table 11: Non-exhaustive list of reviews dealing with aggregation or agglomeration phenomena, in chronological order of publication.

6.4.2. Discrete Element Method (DEM)

Discrete Element Method is a very popular modeling method, but it takes a lot of computing time to implement. Ding et al. [25] is using it to model rocks and coarse aggregates from information gathered using an optical microscope, with the aim of characterizing their morphology in more detail, as this has a major influence on the structure and mechanical behavior of the mixture.

Meanwhile, Spettl et al. [63] uses the discrete element method to model maltodextrin aggregates. In particular, this modeling allows a better understanding of the internal structure of the aggregates, including the coordination number and coordination angle of the primary particles, as well as the porosity of the object. The results are analyzed and compared with real data collected by X-ray tomography, with a relatively small error.

7. Reviews

One of the selection criteria (C7) states that review articles are not to be considered when compiling the set of research articles to be studied for the systematic literature review. However, the subject is so broad and rich that many articles do not meet condition C7, although they are of great interest. In this section, a selection of review articles dealing with aggregates and/or agglomerates are presented and listed in Table 11.

8. Conclusion & Recommendations

The morphological characterization of aggregates or agglomerates using image analysis is a vast and increasingly active field, thanks to the considerable increase in computer processing power over the last 20 years. It is a multidisciplinary subject, ranging from the food industry to the oil industry, from the biomedical field to the chemical industry. In fact, the morphology of the aggregates studied has a great influence on their physico-chemical properties and on the quality of the composite materials that use them.

The method chosen for this review, namely SLR, highlighted several points. First, although virtually all research fields are represented, the chemical industry and environmental engineering seem to be the most active fields when it comes to characterizing the morphology of aggregates or agglomerates by image analysis. Second, many image analysis techniques can be applied regardless of the type and size of the objects being studied. The largest objects are typically rocks and coarse aggregates, for example, in civil engineering and materials science. For the smallest aggregates, soot and aerosol aggregates are the most studied, mainly because of their impact on health and the environment. The fourth point relates to imaging devices and the fact that electron microscopy is over-represented compared to light microscopy. However, again, many of the image analysis techniques and characteristics studied are independent of the type of imaging device used.

The next point concerns the morphological characteristics themselves. It's quite clear that the choice of characteristics studied is correlated with the field of research, the size of the objects, and their nature. In fact, it has become clear that certain characteristics, such as fractal dimension and radius of gyration, only concern very small aggregates and are rarely considered at millimeter scales. Conversely, many morphological properties, such as texture and structure, are generally only mentioned at the highest scales. An important point, however, is the cruel lack of coherence and consistency in the choice of definitions and naming of morphological properties. In fact, there are no less than five definitions of total length, seven definitions of elongation, which seem to be rather simple concepts, at least six definitions of fractal dimension, ten definitions of sphericity, and six definitions of concavity. Not to mention the fact that some definitions are used to describe different properties depending on the author and vice versa. Thus, without being able to define a standard or a norm, it seems appropriate to recommend that each author define the terms to which he refers when mentioning a morphological property.

In the same vein, and despite the fact that all the articles studied deal with image analysis, it's actually quite rare for authors to explain how the various morphological characteristics have been measured. In fact, while imaging devices are often mentioned in detail, the way in which images are processed, segmented and/or binarized is often overlooked. This is very unfortunate, because in order to make the results reproducible, it would be a good idea to always mention at least the program, language or technique used to transform the raw image into one on which it is possible to perform measurements of morphological characteristics.

Another point concerns the emergence of machine learning and deep learning techniques, either for automatic segmentation of images or for their processing with the aim of automatic classification or prediction of morphological characteristics, for example. These techniques generally allow real-time processing, despite a training phase that can be very long and costly in terms of computing power, and are therefore particularly well suited to quality control in the food and pharmaceutical industries. Moreover, just as machine learning or deep learning techniques require large data sets for training, it's worth remembering that a significant amount of data is needed to obtain reliable statistics when calculating averages or standard deviations. In fact, many studies are based on less than a dozen images, usually from electron microscopy, and the observation of a few dozen aggregates or agglomerates to calculate size or shape densities and corresponding means. At the very least, it would be relevant to discuss the validity of the approach on such a small volume of data.

A final point concerns the increasing use of non-destructive techniques (AFM, HIM, etc.) among imaging devices, which not only preserve the physical integrity of the sample under study, but above all ensure that the measuring device does not influence the measurements themselves. It is also noteworthy that while image analysis has often been used as a complement to other techniques, such as laser or X-ray scattering, the imaging devices and techniques used are now proving to be accurate enough to stand on their own when it comes to characterizing the morphology of aggregates or agglomerates.

9. Acknowledgment

The author(s) acknowledge(s) the support of the French Agence Nationale de la Recherche (ANR), under grant ANR-20-CE07-0025 (MORPHING project).

10. Nomenclature

Name	Definition
Ω_1	Robustness
Φ_S	Sphericity
ε	Porosity
A_f	Fractal area
AF	Angularity factor
AFM	Atomic force microscope
AI	Angularity index
ANN	Artificial neural network
A_p	Projected area
a_p	Mean projected area of the primary particles
AR	Aspect ratio
C	Circularity
CAV	Concavity
CNN	Convolutional neural network
CO	Convexity
Cryo-TEM	Cryogenic transmission electron microscope
CT	X-ray computed tomography
d	Diameter of the primary particles
D_e	Euclidean dimension
DEM	Discrete element method
D_{eq}	Equivalent circle diameter
$D_{\mathrm{S,eq}}$	Equivalent spherical diameter
D_f	Fractal dimension
DFA	Discriminant factorial analysis
E	Elongation
Ec	Eccentricity
ECD	Equivalent circle diameter
EM	Electron microscopy
ESD	Equivalent spherical diameter
ESEM	Environmental scanning electron microscope
F	Feret diameter
f_{flat}	Flatness
FE-SEM	Field emission scanning electron microscope
FTI	Fourier transform interferometry
GAN	Generative adversarial networks
H	Height
HR-TEM	High-resolution transmission electron microscope
k	Prefactor
L	Length
LCFM	Laser confocal fluorescence Microscope
N_p	Number of primary particles
O	Compactness
OM	Optical microscopy
P	Perimeter
PCA	Principal component analysis
PGF	Plane geometry factor
PSD	Particle size distribution
PTA	Particle tracking analysis
R	Roundness
R_{circ}	Circumscribed circle radius
R_{in}	Inscribed circle radius
R_g	Radius of gyration
RO	Roughness
S	Surface area
S_D	Sphericity
SAR	Section aspect ratio
SEM	Scanning electron microscope
SF	Shape factor
Si	Simplicity
SLD	Solidity
S_p	Specific surface area
SVM	Support vector machine
T	Thickness
TEM	Transmission electron microscope
TF	Texture Factor
Tx	Texture
V	Volume
W	Width
Wet-SEM	Environmental scanning electron microscope
X	Anisotropy
XMT	X-ray micro-tomography
Y	Complexity
Z	Coverage ratio

Table 12: List of terms and abbreviations used in this article.

Complete list of selected research papers

Year	Reference	Title
1988	Tohno and Takahashi [75]	Shape Analysis of Particles by an Image Scanner and a Microcomputer: Application to Agglomerated Aerosol Particles
1994	Einar Kruis et al. [106]	Characterization of Agglomerated and Aggregated Aerosol Particles Using Image Analysis
1995	Ramachandran and Reist [38]	Characterization of Morphological Changes in Agglomerates Subject to Condensation and Evaporation Using Multiple Fractal Dimensions
1995	Tai and Chen [111]	Nucleation, agglomeration and crystal morphology of calcium carbonate
1996	Stine et al. [70]	The nanometer-scale structure of amyloid-beta visualized by atomic force
1997	Bower et al. [104]	The use of image analysis to characterize aggregates in a shear field
1997	Bernard-Michel et al. [76]	Classification of Crystal Shape Using Fourier Descriptors and Mathematical Morphology
1998	Ortega-Vinuesa et al. [90]	Aggregation of HSA, IgG, and Fibrinogen on Methylated Silicon Surfaces
1998	Vučak et al. [77]	Effect of precipitation conditions on the morphology of calcium carbonate: quantification of crystal shapes using image analysis
1998	Kuo et al. [20]	Morphological Study of Coarse Aggregates Using Image Analysis
1998	Persson [19]	Image analysis of shape and size of fine aggregates
1999	Tang et al. [59]	Characterising latex particles and fractal aggregates using image analysis
2000	Blandin et al. [138]	Using In Situ Image Analysis to Study the Kinetics of Agglomeration in Suspension
2000	Liao et al. [61]	Brownian Dynamics Simulation of Film Formation of Mixed Polymer Latex in the Water Evaporation Stage
2000	Machinski et al. [139]	An Image Analysis Technique for Assessing Particle Size and Agglomeration Tendency of Slurries
2000	Liu et al. [21]	Evaluating Angularity of Coarse Aggregates Using the Virtual Cutting Method Based on 3D Point Cloud Images
2001	Frances et al. [112]	Particle morphology of ground gibbsite in different grinding environments
2001	da Motta et al. [140]	Automated monitoring of activated sludge in a pilot plant using image
2001	Yazicioglu et al. [43]	Measurement of fractal properties of soot agglomerates in laminar coflow diffusion flames using thermophoretic sampling in conjunction with transmission electron microscopy and image processing
2002	Weinbruch et al. [107]	The heterogeneous composition of working place aerosols in a nickel refinery: a transmission and scanning electron microscope study
2002	Pons et al. [78]	Morphological analysis of pharmaceutical powders
2003	Ålander et al. [11]	Characterization of paracetamol agglomerates by image analysis and strength measurement
2003	Wentzel et al. [37]	Transmission electron microscopical and aerosol dynamical characterization of soot aerosols
2003	Tanaka et al. [74]	Direct observation of aggregates and agglomerates in alumina granules
2003	Faria et al. [86]	Quantification of the morphology of sucrose crystals by image analysis
2003	Blandin et al. [141]	Agglomeration in suspension of salicylic acid fine particles: influence of some process parameters on kinetics and agglomerate final size
2004	Liu et al. [71]	Residues 17-20 and 30-35 of beta-amyloid play critical roles in aggregation
2004	Hoyer et al. [68]	Rapid Self-assembly of α-Synuclein Observed by In Situ Atomic Force Microscopy
2005	Jansen et al. [72]	Amyloidogenic Self-Assembly of Insulin Aggregates Probed by High Resolution Atomic Force Microscopy
2005	Pons et al. [79]	Comparison of methods for the characterisation by image analysis of crystalline agglomerates: The case of gibbsite
2005	Blandin et al. [142]	Modelling of agglomeration in suspension: Application to salicylic acid microparticles
2006	Lapuerta et al. [39]	A method to determine the fractal dimension of diesel soot agglomerates
2006	Neer and Koylu [44]	Effect of operating conditions on the size, morphology, and concentration of submicrometer particulates emitted from a diesel engine
2006	Zhang et al. [56]	Optical trapping and light-induced agglomeration of gold nanoparticle aggregates
2006	Apetri et al. [69]	Secondary Structure of α-Synuclein Oligomers: Characterization by Raman and Atomic Force Microscopy
2006	Jenneson and Gundogdu [96]	In situ x-ray imaging of nanoparticle agglomeration in fluidized beds
2006	Subero-Couroyer et al. [143]	Agglomeration in suspension of salicylic acid fine particles: Analysis of the wetting period and effect of the binder injection mode on the final agglomerate size
2007	Dai et al. [55]	Vacuum metal deposition: visualisation of gold agglomerates using TEM imaging
2007	Martínez-Pedrero et al. [60]	Structure and stability of aggregates formed by electrical double-layered magnetic particles
2007	Manno et al. [67]	Kinetics of Different Processes in Human Insulin Amyloid Formation
2008	Huang et al. [144]	Substrate morphology induced self-organization into carbon nanotube arrays, ropes, and agglomerates
2008	Cameirão et al. [4]	Effect of precipitation conditions on the morphology of strontium molybdate agglomerates
2008	Li et al. [145]	Measurement of drug agglomerates in powder blending simulation samples by near infrared chemical imaging
2009	Shen et al. [146]	Nanospheres of silver nanoparticles: agglomeration, surface morphology control and application as SERS substrates
2009	Luo et al. [45]	Morphological and semi-quantitative characteristics of diesel soot agglomerates emitted from commercial vehicles and a dynamometer
2009	Ershov et al. [80]	Methods of handling of in-bulk agglomeration layer image representation for granulometric composition assessment
2009	Turchiuli and Castillo-Castaneda [87]	Agglomerates Structure Characterization Using 3D-Image Reconstruction
2010	Shin et al. [102]	The effect of particle morphology on unipolar diffusion charging of nanoparticle agglomerates in the transition regime
2010	Horst et al. [52]	Dispersion of TiO2 Nanoparticle Agglomerates by Pseudomonas aeruginosa
2010	Kierys et al. [1]	The porosity and morphology of mesoporous silica agglomerates
2010	Adamcik et al. [73]	Understanding amyloid aggregation by statistical analysis of atomic force microscopy images
2011	Maggi et al. [94]	Agglomeration in solid rocket propellants: novel experimental and modeling methods
2011	Menzer et al. [147]	Percolation behaviour of multiwalled carbon nanotubes of altered length and primary agglomerate morphology in melt mixed isotactic polypropylene-based composites
2012	Long et al. [2]	Novel issues of morphology, size, and structure of Pt nanoparticles in chemical engineering: surface attachment, aggregation or agglomeration, assembly, and structural changes
2012	De Temmerman et al. [103]	Quantitative characterization of agglomerates and aggregates of pyrogenic and precipitated amorphous silica nanomaterials by transmission electron microscopy
2012	De Iuliis et al. [40]	Effect of hydrogen addition on soot formation in an ethylene/air premixed flame
2012	Lakshminarasimhan et al. [53]	Effect of Agglomerated State in Mesoporous TiO2 on the Morphology of Photodeposited Pt and Photocatalytic Activity
2012	Ono et al. [148]	Influence of furnace temperature and residence time on configurations of carbon black
2012	Cai et al. [149]	Morphology evolution of immiscible polymer blends as directed by nanoparticle self-agglomeration
2012	Dadkhah et al. [150]	Characterization of the internal morphology of agglomerates produced in a spray fluidized bed by X-ray tomography
2013	Neef et al. [99]	Morphology and Agglomeration Control of LiMnPO4 Micro- and Nanocrystals
2013	Born and Kraus [109]	Ligand-dominated temperature dependence of agglomeration kinetics and morphology in alkyl-thiol-coated gold nanoparticles
2013	Ono et al. [151]	Effect of benzene–acetylene compositions on carbon black configurations produced by benzene pyrolysis
2013	Schenk et al. [41]	Imaging Nanocarbon Materials: Soot Particles in Flames are Not Structurally Homogeneous
2013	Dacanal et al. [88]	Fluid dynamics and morphological characterization of soy protein isolate particles obtained by agglomeration in pulsed-fluid bed
2014	Høydalsvik et al. [152]	In situ X-ray ptychography imaging of high-temperature CO2 acceptor particle agglomerates
2014	Dadkhah and Tsotsas [153]	Study of the morphology of solidified binder in spray fluidized bed agglomerates by X-ray tomography
2014	Vissotto et al. [89]	Morphological characterization with image analysis of cocoa beverage powder agglomerated with steam
2014	Fernandez Martinez et al. [81]	Use of decision tree models based on evolutionary algorithms for the morphological classification of reinforcing nano-particle aggregates
2015	Frieke Kuper et al. [12]	Toxicity assessment of aggregated/agglomerated cerium oxide nanoparticles in an in vitro 3D airway model: The influence of mucociliary clearance

Year	Reference	Title
2015	Yang et al. [154]	Morphology of Hydrophobic Agglomerates of Molybdenite Fines in Aqueous Suspensions
2015	Ochsenbein et al. [120]	Agglomeration of Needle-like Crystals in Suspension: I. Measurements
2015	Ghabchi et al. [22]	Effect of Shape Parameters and Gradation on Laboratory-Measured Permeability of Aggregate Bases
2016	Bai et al. [155]	Tailoring film agglomeration for preparation of silver nanoparticles with controlled morphology
2016	Razavi-Nouri et al. [14]	Effect of Organoclay Ordering and Agglomeration on Morphology and Mechanical Properties of Uncured and Dynamically Cured Ethylene-Octene Copolymer Nanocomposites
2016	Razavi-Nouri et al. [14]	Effect of Organoclay Ordering and Agglomeration on Morphology and Mechanical Properties of Uncured and Dynamically Cured Ethylene-Octene Copolymer Nanocomposites
2016	Kong et al. [92]	Morphological changes of nano-Al agglomerates during reaction and its effect on combustion
2016	Abdellatif et al. [57]	Fractal analysis of inter-particle interaction forces in gold nanoparticle aggregates
2016	Pashminehazar et al. [64]	Three dimensional characterization of morphology and internal structure of soft material agglomerates produced in spray fluidized bed by X-ray tomography
2016	Chen et al. [156]	Agglomeration process of surfactant-dispersed carbon nanotubes in unstable dispersion: A two-stage agglomeration model and experimental evidence
2016	Huo et al. [121]	In-situ crystal morphology identification using imaging analysis with application to the L-glutamic acid crystallization
2016	Spettl et al. [63]	Bonded-particle extraction and stochastic modeling of internal agglomerate structures
2016	Liu et al. [23]	Quantification of Aggregate Morphologic Characteristics as Related to Mechanical Properties of Asphalt Concrete with Improved FTI System
2016	Freyre-Fonseca et al. [50]	Morphological and Physicochemical Characterization of Agglomerates of Titanium Dioxide Nanoparticles in Cell Culture Media
2017	Machado et al. [54]	A complex network approach for nanoparticle agglomeration analysis in nanoscale images
2017	Vasicek et al. [110]	Thermoresponsive nanoparticle agglomeration/aggregation in salt solutions: Dependence on graft density
2017	Kim et al. [100]	Solvent effect on the Nafion agglomerate morphology in the catalyst layer of the proton exchange membrane fuel cells
2017	Lapuerta et al. [91]	Morphological analysis of soot agglomerates from biodiesel surrogates in a coflow burner
2017	Guérin et al. [8]	Dynamics of aggregate size and shape properties under sequenced flocculation in a turbulent Taylor-Couette reactor
2017	Yang et al. [157]	Shear-Assisted Fabrication of Block Copolymer Agglomerates with Various Morphologies in Viscous Medium
2017	Dong et al. [158]	Nanostructure characterization of asphalt-aggregate interface through molecular dynamics simulation and atomic force microscopy
2017	Huo et al. [118]	Online Detection of Particle Agglomeration during Solution Crystallization by Microscopic Double-View Image Analysis
2017	Guarieiro [46]	Investigation on Morphology and Fractal Dimension of Diesel and Diesel-Biodiesel Soot Agglomerates
2017	van Beers et al. [5]	Micro-Flow Imaging as a quantitative tool to assess size and agglomeration of PLGA microparticles
2017	Zou et al. [159]	Image analysis for in-situ detection of agglomeration for needle-like crystals
2017	Mehle et al. [7]	In-line recognition of agglomerated pharmaceutical pellets with density-based clustering and convolutional neural network
2017	Liu et al. [24]	Modelling and evaluation of aggregate morphology on asphalt compression behavior
2017	Ding et al. [25]	Morphological characterization and mechanical analysis for coarse aggregate skeleton of asphalt mixture based on discrete-element modeling
2018	Bartczak et al. [160]	Changes in silica nanoparticles upon internalisation by cells: size, aggregation/agglomeration state, mass- and number-based concentrations
2018	Engelmann et al. [161]	Magnetic Relaxation of Agglomerated and Immobilized Iron Oxide Nanoparticles for Hyperthermia and Imaging Applications
2018	Reyes-Salgado [105]	Study of complex morphology of agglomerations formed by graphite nanoinclusions and its effect on the mechanical properties of the composite materials
2018	Zhang et al. [162]	A new multiple-time-step three-dimensional discrete element modeling of aerosol acoustic agglomeration
2018	Frei and Kruis [82]	Fully automated primary particle size analysis of agglomerates on transmission electron microscopy images via artificial neural networks
2018	Pashminehazar et al. [65]	Spatial morphology of maltodextrin agglomerates from X-ray microtomographic data: Real structure evaluation vs. spherical primary particle model
2018	Mehle et al. [9]	In-line agglomeration degree estimation in fluidized bed pellet coating processes using visual imaging
2018	Jin et al. [26]	Aggregate Shape Characterization Using Virtual Measurement of Three-Dimensional Solid Models Constructed from X-Ray CT Images of Aggregates
2019	Gigone et al. [48]	Soot aggregate morphology in coflow laminar ethylene diffusion flames at elevated pressures
2019	Cetinbas et al. [101]	Effects of Porous Carbon Morphology, Agglomerate Structure and Relative Humidity on Local Oxygen Transport Resistance
2019	Koutny et al. [29]	Packing density modelling of non-spherical aggreg ates for particle composite design
2019	Guérin et al. [6]	Fractal dimensions and morphological characteristics of aggregates formed in different physico-chemical and mechanical flocculation environments
2019	Atalar and Yazici [66]	Effect of different binders on reconstitution behaviors and physical, structural, and morphological properties of fluidized bed agglomerated yoghurt powder
2019	Barustan and Jung [163]	Morphology of Iron and Agglomeration Behaviour During Reduction of Iron Oxide Fines
2019	Li et al. [27]	Three-Dimensional Simulation of Aggregate and Asphalt Mixture Using Parameterized Shape and Size Gradation
2019	Jin et al. [28]	3D Quantification for Aggregate Morphology Using Surface Discretization Based on Solid Modeling
2019	Le Barbenchon et al. [164]	Multi-scale foam : 3D structure/compressive behaviour relationship of agglomerated cork
2020	Weston et al. [165]	Connecting Particle Interactions to Agglomerate Morphology and Rheology of Boehmite Nanocrystal Suspensions
2020	Murugadoss et al. [51]	Agglomeration of titanium dioxide nanoparticles increases toxicological responses in vitro and in vivo
2020	Patiño et al. [49]	Soot primary particle sizing in a n-heptane doped methane/air laminar coflow diffusion flame by planar two-color TiRe-LII and TEM image analysis
2020	Cortés et al. [47]	Effect of Fuels and Oxygen Indices on the Morphology of Soot Generated in Laminar Coflow Diffusion Flames
2020	Huyan et al. [31]	Image-Based Coarse-Aggregate Angularity Analysis and Evaluation
2020	Jin et al. [95]	Three-dimensional spatial distributions of agglomerated particles on and near the burning surface of aluminized solid propellant using morphological digital in-line holography
2020	Lu et al. [166]	Crystal texture recognition system based on image analysis for the analysis of agglomerates
2020	Omar [10]	Experimental investigations of adipic acid agglomeration behavior under different operating conditions using image analysis technique QICPIC software
2020	Frei and Kruis [83]	Image-based size analysis of agglomerated and partially sintered particles via convolutional neural networks
2020	Zhalehrajabi et al. [167]	Modelling of urea aggregation efficiency via particle tracking velocimetry in fluidized bed granulation
2020	Li et al. [30]	Morphology-based indices and recommended sampling sizes for using image-based methods to quantify degradations of compacted aggregate materials
2020	Zhao et al. [32]	A digitalized 2D particle database for statistical shape analysis and discrete modeling of rock aggregate
2021	McCallister et al. [108]	Influence of agglomerate morphology on micro cold spray of Ag nanopowders
2021	Wang et al. [168]	Experimental investigation on the microstructure of fluidized nanoparticle agglomerates by TEM image analysis
2021	Lowe et al. [169]	Fragmentation dynamics of single agglomerate-to-wall impaction
2021	Sung and Abelmann [97]	Agglomeration structure of superparamagnetic nanoparticles in a nematic liquid crystal medium: Image analysis datasets based on cryo-electron microscopy and polarised optical microscopy techniques
2021	Romphophak et al. [170]	Analysis of flocculation in a jet clarifier. Part 2 - Analysis of aggregate size distribution versus Camp number
2021	Kelesidis and Pratsinis [42]	Determination of the volume fraction of soot accounting for its composition and morphology
2021	Wang et al. [33]	Determining the specific surface area of coarse aggregate based on sieving curve via image-analysis approach
2021	Zheleznyakova [34]	A cost-effective computational approach based on molecular dynamics for generating 3D packs of irregularly-shaped grains in a container of complex geometry

Year	Reference	Title
2021	Monchot et al. [84]	Deep Learning Based Instance Segmentation of Titanium Dioxide Particles in the Form of Agglomerates in Scanning Electron Microscopy
2021	Liu et al. [35]	Study on Quantitative Characterization of Morphological Characteristics and High Temperature Performance Evaluation of Coarse Aggregate Based on Computer Vision
2021	Rühle et al. [85]	Workflow towards automated segmentation of agglomerated, non-spherical particles from electron microscopy images using artificial neural networks
2022	Cecil et al. [98]	Nonlinear Agglomeration of Bimodal Colloids under Microgravity
2022	Shen and Zhang [171]	Hydrophobic agglomeration behavior of rhodochrosite fines Co-induced by oleic acid and shearing
2022	Cohen et al. [93]	Agglomeration in Composite Propellants Containing Different Nano-Aluminum Powders
2022	Lins et al. [113]	Potential of Deep Learning Methods for Deep Level Particle Characterization in Crystallization
2022	Müller et al. [172]	From spores to fungal pellets: A new high-throughput image analysis highlights the structural development of Aspergillus niger
2022	Kamani and Ajalloeian [36]	Investigation of the changes in aggregate morphology during different aggregate abrasion/degradation tests using image analysis
2023	Zhang et al. [173]	Liquid Cohesion Induced Particle Agglomeration Enhances Clogging in Rock Fractures
2023	Theodon et al. [62]	GRAPE: A Stochastic Geometrical 3D Model for Aggregates of Particles With Tunable 2D Morphological Projected Properties

Table 13: Comprehensive list of research papers selected for this SLR, sorted in order of publication.

References

[1] A. Kierys, W. Buda, J. Goworek, The porosity and morphology of mesoporous silica agglomerates, Journal of Porous Materials 17 (2010) 669–676. URL: https://doi.org/10.1007/s10934-009-9337-9. doi:10.1007/s10934-009-9337-9.

[2] N. V. Long, C. M. Thi, M. Nogami, M. Ohtaki, Novel issues of morphology, size, and structure of pt nanoparticles in chemical engineering: surface attachment, aggregation or agglomeration, assembly, and structural changes, New J. Chem. 36 (2012) 1320–1334. URL: http://dx.doi.org/10.1039/C2NJ40027H. doi:10.1039/C2NJ40027H.

[3] H. Wang, A. Pietrasanta, D. Jeulin, F. Willot, M. Faessel, L. Sorbier, M. Moreaud, Modelling mesoporous alumina microstructure with 3d random models of platelets, Journal of Microscopy 260 (2015) 287–301. URL: https://onlinelibrary.wiley.com/doi/abs/10.1111/jmi.12295. doi:https://doi.org/10.1111/jmi.12295. arXiv:https://onlinelibrary.wiley.com/doi/pdf/10.1111/jmi.12295.

[4] A. Cameirão, R. David, F. Espitalier, F. Gruy, Effect of precipitation conditions on the morphology of strontium molybdate agglomerates, Journal of Crystal Growth 310 (2008) 4152–4162. URL: https://www.sciencedirect.com/science/article/pii/S0022024808004831. doi:https://doi.org/10.1016/j.jcrysgro.2008.06.024.

[5] M. M. van Beers, C. Slooten, J. Meulenaar, A. S. Sediq, R. Verrijk, W. Jiskoot, Micro-flow imaging as a quantitative tool to assess size and agglomeration of plga microparticles, European Journal of Pharmaceutics and Biopharmaceutics 117 (2017) 91–104. URL: https://www.sciencedirect.com/science/article/pii/S0939641117301236. doi:https://doi.org/10.1016/j.ejpb.2017.04.002.

[6] L. Guérin, C. Frances, A. Liné, C. Coufort-Saudejaud, Fractal dimensions and morphological characteristics of aggregates formed in different physico-chemical and mechanical flocculation environments, Colloids and Surfaces A: Physicochemical and Engineering Aspects 560 (2019) 213–222. URL: https://www.sciencedirect.com/science/article/pii/S0927775718313153. doi:https://doi.org/10.1016/j.colsurfa.2018.10.017.

[7] A. Mehle, B. Likar, D. Tomaževič, In-line recognition of agglomerated pharmaceutical pellets with density-based clustering and convolutional neural network, in: 2017 Fifteenth IAPR International Conference on Machine Vision Applications (MVA), 2017, pp. 9–12. doi:10.23919/MVA.2017.7986760.

[8] L. Guérin, C. Coufort-Saudejaud, A. Liné, C. Frances, Dynamics of aggregate size and shape properties under sequenced flocculation in a turbulent taylor-couette reactor, Journal of Colloid and Interface Science 491 (2017) 167–178. URL: https://www.sciencedirect.com/science/article/pii/S0021979716310426. doi:https://doi.org/10.1016/j.jcis.2016.12.042.

[9] A. Mehle, D. Kitak, G. Podrekar, B. Likar, D. Tomaževič, In-line agglomeration degree estimation in fluidized bed pellet coating processes using visual imaging, International Journal of Pharmaceutics 546 (2018) 78–85. URL: https://www.sciencedirect.com/science/article/pii/S0378517318303223. doi:https://doi.org/10.1016/j.ijpharm.2018.05.024.

[10] W. Omar, Experimental investigations of adipic acid agglomeration behavior under different operating conditions using image analysis technique qicpic software, Particulate Science and Technology 38 (2020) 740–746. URL: https://doi.org/10.1080/02726351.2019.1620386. doi:10.1080/02726351.2019.1620386. arXiv:https://doi.org/10.1080/02726351.2019.1620386.

[11] E. M. Ålander, M. S. Uusi-Penttilä, Åke C Rasmuson, Characterization of paracetamol agglomerates by image analysis and strength measurement, Powder Technology 130 (2003) 298–306. URL: https://www.sciencedirect.com/science/article/pii/S0032591002002085. doi:https://doi.org/10.1016/S0032-5910(02)00208-5.

[12] C. Frieke Kuper, M. Gröllers-Mulderij, T. Maarschalkerweerd, N. M. Meulendijks, A. Reus, F. van Acker, E. K. Zondervan-van den Beuken, M. E. Wouters, S. Bijlsma, I. M. Kooter, Toxicity assessment of aggregated/agglomerated cerium oxide nanoparticles in an in vitro 3d airway model: The influence of mucociliary clearance, Toxicology in Vitro 29 (2015) 389–397. URL: https://www.sciencedirect.com/science/article/pii/S0887233314002082. doi:https://doi.org/10.1016/j.tiv.2014.10.017.

[13] Z. Du, Q. Zhu, C. Fan, F. Pan, H. Li, Z. Xie, Influence of reduction condition on the morphology of newly formed metallic iron during the fluidized bed reduction of fine iron ores and its corresponding agglomeration behavior, steel research international 87 (2016) 789–797. URL: https://onlinelibrary.wiley.com/doi/abs/10.1002/srin.201500240. doi:https://doi.org/10.1002/srin.201500240. arXiv:https://onlinelibrary.wiley.com/doi/pdf/10.1002/srin.2015

[14] M. Razavi-Nouri, A. Sabet, M. Tayefi, M. Imeni, Effect of organoclay ordering and agglomeration on morphology and mechanical properties of uncured and dynamically cured ethylene-octene copolymer nanocomposites, Macromolecular Materials and Engineering 301 (2016) 1513–1524. URL: https://onlinelibrary.wiley.com/doi/abs/10.1002/mame.201600255. doi:https://doi.org/10.1002/mame.201600255. arXiv:https://onlinelibrary.wiley.com/doi/pdf/10.1002/mame.2016

[15] P. F. Fewster, The limits of x-ray diffraction theory, Crystals 13 (2023). URL: https://www.mdpi.com/2073-4352/13/3/521. doi:10.3390/cryst13030521.

[16] M. J. Grant, A. Booth, A typology of reviews: an analysis of 14 review types and associated methodologies, Health Information & Libraries Journal 26 (2009) 91–108. URL: https://onlinelibrary.wiley.com/doi/abs/10.1111/j.1471-1842.2009.00848.x. doi:https://doi.org/10.1111/j.1471-1842.2009.00848.x. arXiv:https://onlinelibrary.wiley.com/doi/pdf/10.1111/j.1471-18

[17] B. A. Kitchenham, S. Charters, Guidelines for performing Systematic Literature Reviews in Software Engineering, Technical Report EBSE 2007-001, Keele University and Durham University Joint Report, 2007. URL: https://www.elsevier.com/__data/promis_misc/525444systematicreviewsguide.pdf.

[18] G. Nichols, S. Byard, M. J. Bloxham, J. Botterill, N. J. Dawson, A. Dennis, V. Diart, N. C. North, J. D. Sherwood, A review of the terms agglomerate and aggregate with a recommendation for nomenclature used in powder and particle characterization, Journal of Pharmaceutical Sciences 91 (2002) 2103–2109. URL: https://www.sciencedirect.com/science/article/pii/S0022354916310942. doi:https://doi.org/10.1002/jps.10191.

[19] A.-L. Persson, Image analysis of shape and size of fine aggregates, Engineering Geology 50 (1998) 177–186. URL: https://www.sciencedirect.com/science/article/pii/S001379529800009X. doi:https://doi.org/10.1016/S0013-7952(98)00009-X.

[20] C.-Y. Kuo, R. S. Rollings, L. N. Lynch, Morphological study of coarse aggregates using image analysis, Journal of Materials in Civil Engineering 10 (1998) 135–142. doi:10.1061/(ASCE)0899-1561(1998)10:3(135).

[21] H. Liu, Z. Sun, W. Li, J. Huyan, M. Guo, X. Hao, Evaluating angularity of coarse aggregates using the virtual cutting method based on 3d point cloud images, IEEE Access 8 (2020) 143241–143255. doi:10.1109/ACCESS.2020.3013901.

[22] R. Ghabchi, M. Zaman, H. Kazmee, D. Singh, Effect of shape parameters and gradation on laboratory-measured permeability of aggregate bases, International Journal of Geomechanics 15 (2015) 04014070. doi:10.1061/(ASCE)GM.1943-5622.0000397.

[23] Y. Liu, W. Sun, H. Nair, D. S. Lane, L. Wang, Quantification of aggregate morphologic characteristics as related to mechanical properties of asphalt concrete with improved fti system, Journal of Materials in Civil Engineering 28 (2016) 04016046. doi:10.1061/(ASCE)MT.1943-5533.0001535.

[24] P. Liu, J. Hu, D. Wang, M. Oeser, S. Alber, W. Ressel, G. Canon Falla, Modelling and evaluation of aggregate morphology on asphalt compression behavior, Construction and Building Materials 133 (2017) 196–208. URL: https://www.sciencedirect.com/science/article/pii/S095006181631947X. doi:https://doi.org/10.1016/j.conbuildmat.2016.12.041.

[25] X. Ding, T. Ma, W. Gao, Morphological characterization and mechanical analysis for coarse aggregate skeleton of asphalt mixture based on discrete-element modeling, Construction and Building Materials 154 (2017) 1048–1061. URL: https://www.sciencedirect.com/science/article/pii/S0950061817315994. doi:https://doi.org/10.1016/j.conbuildmat.2017.08.008.

[26] C. Jin, X. Yang, Z. You, K. Liu, Aggregate shape characterization using virtual measurement of three-dimensional solid models constructed from x-ray ct images of aggregates, Journal of Materials in Civil Engineering 30 (2018) 04018026. doi:10.1061/(ASCE)MT.1943-5533.0002210.

[27] J. Li, J. Zhang, G. Qian, J. Zheng, Y. Zhang, Three-dimensional simulation of aggregate and asphalt mixture using parameterized shape and size gradation, Journal of Materials in Civil Engineering 31 (2019) 04019004. doi:10.1061/(ASCE)MT.1943-5533.0002623.

[28] C. Jin, F. Zou, X. Yang, Z. You, 3d quantification for aggregate morphology using surface discretization based on solid modeling, Journal of Materials in Civil Engineering 31 (2019) 04019123. doi:10.1061/(ASCE)MT.1943-5533.0002766.

[29] O. Koutny, J. Kratochvil, M. Drdlova, E. Bystrianska, Packing density modelling of non-spherical aggreg ates for particle composite design, IOP Conference Series: Materials Science and Engineering 583 (2019) 012013. URL: https://dx.doi.org/10.1088/1757-899X/583/1/012013. doi:10.1088/1757-899X/583/1/012013.

[30] C. Li, J. Zheng, Z. Zhang, A. Sha, J. Li, Morphology-based indices and recommended sampling sizes for using image-based methods to quantify degradations of compacted aggregate materials, Construction and Building Materials 230 (2020) 116970. URL: https://www.sciencedirect.com/science/article/pii/S0950061819324122. doi:https://doi.org/10.1016/j.conbuildmat.2019.116970.

[31] J. Huyan, W. Li, S. Tighe, Y. Zhang, B. Yue, Image-based coarse-aggregate angularity analysis and evaluation, Journal of Materials in Civil Engineering 32 (2020) 04020140. doi:10.1061/(ASCE)MT.1943-5533.0003150.

[32] L. Zhao, S. Zhang, D. Huang, X. Wang, A digitalized 2d particle database for statistical shape analysis and discrete modeling of rock aggregate, Construction and Building Materials 247 (2020) 117906. URL: https://www.sciencedirect.com/science/article/pii/S0950061819333598. doi:https://doi.org/10.1016/j.conbuildmat.2019.117906.

[33] Q. Wang, J. He, J. Sun, J. Ho, Determining the specific surface area of coarse aggregate based on sieving curve via image-analysis approach, Construction and Building Materials 305 (2021) 124728. URL: https://www.sciencedirect.com/science/article/pii/S0950061821024831. doi:https://doi.org/10.1016/j.conbuildmat.2021.124728.

[34] A. L. Zheleznyakova, A cost-effective computational approach based on molecular dynamics for generating 3d packs of irregularly-shaped grains in a container of complex geometry, Powder Technology 394 (2021) 403–423. URL: https://www.sciencedirect.com/science/article/pii/S0032591021007579. doi:https://doi.org/10.1016/j.powtec.2021.08.070.

[35] Z. Liu, C. Zhang, L. Shao, J. Wang, Study on quantitative characterization of morphological characteristics and high temperature performance evaluation of coarse aggregate based on computer vision, Frontiers in Materials 7 (2021). URL: https://www.frontiersin.org/articles/10.3389/fmats.2020.607105. doi:10.3389/fmats.2020.607105.

[36] M. Kamani, R. Ajalloeian, Investigation of the changes in aggregate morphology during different aggregate abrasion/degradation tests using image analysis, Construction and Building Materials 314 (2022) 125614. URL: https://www.sciencedirect.com/science/article/pii/S0950061821033511. doi:https://doi.org/10.1016/j.conbuildmat.2021.125614.

[37] M. Wentzel, H. Gorzawski, K.-H. Naumann, H. Saathoff, S. Weinbruch, Transmission electron microscopical and aerosol dynamical characterization of soot aerosols, Journal of Aerosol Science 34 (2003) 1347–1370. URL: https://www.sciencedirect.com/science/article/pii/S0021850203003604. doi:https://doi.org/10.1016/S0021-8502(03)00360-4, intercomparison of Soot Measurement Techniques.

[38] G. Ramachandran, P. C. Reist, Characterization of morphological changes in agglomerates subject to condensation and evaporation using multiple fractal dimensions, Aerosol Science and Technology 23 (1995) 431–442. URL: https://doi.org/10.1080/02786829508965326. doi:10.1080/02786829508965326. arXiv:https://doi.org/10.1080/02786829508965326.

[39] M. Lapuerta, R. Ballesteros, F. J. Martos, A method to determine the fractal dimension of diesel soot agglomerates, Journal of Colloid and Interface Science 303 (2006) 149–158. URL: https://www.sciencedirect.com/science/article/pii/S0021979706006382. doi:https://doi.org/10.1016/j.jcis.2006.07.066.

[40] S. De Iuliis, S. Maffi, F. Migliorini, F. Cignoli, G. Zizak, Effect of hydrogen addition on soot formation in an ethylene/air premixed flame, Applied Physics B 106 (2012) 707–715. URL: https://doi.org/10.1007/s00340-012-4903-2. doi:10.1007/s00340-012-4903-2.

[41] M. Schenk, S. Lieb, H. Vieker, A. Beyer, A. Gölzhäuser, H. Wang, K. Kohse-Höinghaus, Imaging nanocarbon materials: Soot particles in flames are not structurally homogeneous, ChemPhysChem 14 (2013) 3248–3254. URL: https://chemistry-europe.onlinelibrary.wiley.com/doi/abs/10.1002/cphc.201300581. doi:https://doi.org/10.1002/cphc.201300581. arXiv:https://chemistry-europe.onlinelibrary.wiley.com/doi/pdf/

[42] G. A. Kelesidis, S. E. Pratsinis, Determination of the volume fraction of soot accounting for its composition and morphology, Proceedings of the Combustion Institute 38 (2021) 1189–1196. URL: https://www.sciencedirect.com/science/article/pii/S1540748920304879. doi:https://doi.org/10.1016/j.proci.2020.07.055.

[43] A. G. Yazicioglu, C. M. Megaridis, A. Campbell, K.-O. Lee, M. Y. Choi, Measurement of fractal properties of soot agglomerates in laminar coflow diffusion flames using thermophoretic sampling in conjunction with transmission electron microscopy and image processing, Combustion Science and Technology 171 (2001) 71–87. URL: https://doi.org/10.1080/00102200108907859. doi:10.1080/00102200108907859. arXiv:https://doi.org/10.1080/00102200108907859.

[44] A. Neer, U. O. Koylu, Effect of operating conditions on the size, morphology, and concentration of submicrometer particulates emitted from a diesel engine, Combustion and Flame 146 (2006) 142–154. URL: https://www.sciencedirect.com/science/article/pii/S0010218006001088. doi:https://doi.

org/10.1016/j.combustflame.2006.04.003.

[45] C.-H. Luo, W.-M. Lee, J.-J. Liaw, Morphological and semi-quantitative characteristics of diesel soot agglomerates emitted from commercial vehicles and a dynamometer, Journal of Environmental Sciences 21 (2009) 452–457. URL: https://www.sciencedirect.com/science/article/pii/S1001074208622913. doi:https://doi.org/10.1016/S1001-0742(08)62291-3.

[46] A. L. N. Guarieiro, An investigation on morphology and fractal dimension of diesel and Diesel-Biodiesel soot agglomerates, 2017.

[47] D. Cortés, J. Morán, F. Liu, F. Escudero, J.-L. Consalvi, A. Fuentes, Effect of fuels and oxygen indices on the morphology of soot generated in laminar coflow diffusion flames, Energy & Fuels 32 (2018) 11802–11813. URL: https://doi.org/10.1021/acs.energyfuels.8b01301. doi:10.1021/acs.energyfuels.8b01301.

[48] B. Gigone, A. E. Karataş, Ömer L. Gülder, Soot aggregate morphology in coflow laminar ethylene diffusion flames at elevated pressures, Proceedings of the Combustion Institute 37 (2019) 841–848. URL: https://www.sciencedirect.com/science/article/pii/S1540748918302864. doi:https://doi.org/10.1016/j.proci.2018.06.103.

[49] F. Patiño, J. Cruz, I. Verdugo, J. Morán, J. Consalvi, F. Liu, X. Du, A. Fuentes, Soot primary particle sizing in a n-heptane doped methane/air laminar coflow diffusion flame by planar two-color tire-lii and tem image analysis, Fuel 266 (2020) 117030. URL: https://www.sciencedirect.com/science/article/pii/S0016236120300259. doi:https://doi.org/10.1016/j.fuel.2020.117030.

[50] V. Freyre-Fonseca, D. I. Téllez-Medina, E. I. Medina-Reyes, M. Cornejo-Mazón, E. O. López-Villegas, L. Alamilla-Beltrán, J. Ocotlán-Flores, Y. I. Chirino, G. F. Gutiérrez-López, Morphological and physicochemical characterization of agglomerates of titanium dioxide nanoparticles in cell culture media, Journal of Nanomaterials 2016 (2016) 5937932. URL: https://doi.org/10.1155/2016/5937932. doi:10.1155/2016/5937932.

[51] S. Murugadoss, F. Brassinne, N. Sebaihi, J. Petry, S. M. Cokic, K. L. Van Landuyt, L. Godderis, J. Mast, D. Lison, P. H. Hoet, S. van den Brule, Agglomeration of titanium dioxide nanoparticles increases toxicological responses in vitro and in vivo, Particle and Fibre Toxicology 17 (2020) 10. URL: https://doi.org/10.1186/s12989-020-00341-7. doi:10.1186/s12989-020-00341-7.

[52] A. M. Horst, A. C. Neal, R. E. Mielke, P. R. Sislian, W. H. Suh, L. Mädler, G. D. Stucky, P. A. Holden, Dispersion of tio2 nanoparticle agglomerates by pseudomonas aeruginosa, Applied and Environmental Microbiology 76 (2010) 7292–7298. URL: https://journals.asm.org/doi/abs/10.1128/AEM.00324-10. doi:10.1128/AEM.00324-10. arXiv:https://journals.asm.org/doi/pdf/10.1128/AEM.00324-10.

[53] N. Lakshminarasimhan, A. D. Bokare, W. Choi, Effect of agglomerated state in mesoporous tio2 on the morphology of photodeposited pt and photocatalytic activity, The Journal of Physical Chemistry C 116 (2012) 17531–17539. URL: https://doi.org/10.1021/jp303118q. doi:10.1021/jp303118q.

[54] B. B. Machado, L. F. Scabini, J. P. Margarido Orue, M. S. de Arruda, D. N. Goncalves, W. N. Goncalves, R. Moreira, J. F. Rodrigues-Jr, A complex network approach for nanoparticle agglomeration analysis in nanoscale images, Journal of Nanoparticle Research 19 (2017) 65. URL: https://doi.org/10.1007/s11051-017-3760-7. doi:10.1007/s11051-017-3760-7.

[55] X. Dai, M. Stoilovic, C. Lennard, N. Speers, Vacuum metal deposition: Visualisation of gold agglomerates using tem imaging, Forensic Science International 168 (2007) 219–222. URL: https://www.sciencedirect.com/science/article/pii/S0379073806000284. doi:https://doi.org/10.1016/j.forsciint.2006.01.012.

[56] Y. Zhang, C. Gu, A. M. Schwartzberg, S. Chen, J. Z. Zhang, Optical trapping and light-induced agglomeration of gold nanoparticle aggregates, Phys. Rev. B 73 (2006) 165405. URL: https://link.aps.org/doi/10.1103/PhysRevB.73.165405. doi:10.1103/PhysRevB.73.165405.

[57] M. Abdellatif, G. Abdelrasoul, M. Salerno, I. Liakos, A. Scarpellini, S. Marras, A. Diaspro, Fractal analysis of inter-particle interaction forces in gold nanoparticle aggregates, Colloids and Surfaces A: Physicochemical and Engineering Aspects 497 (2016) 225–232. URL: https://www.sciencedirect.com/science/article/pii/S0927775716301376. doi:https://doi.org/10.1016/j.colsurfa.2016.03.013.

[58] Y.-T. Kim, J. Schilling, S. L. Schweizer, R. B. Wehrspohn, Morphology dependence on surface-enhanced raman scattering using gold nanorod arrays consisting of agglomerated nanoparticles, Plasmonics 12 (2017) 203–208. URL: https://doi.org/10.1007/s11468-016-0250-1. doi:10.1007/s11468-016-0250-1.

[59] S. Tang, C. M. McFarlane, G. C. Paul, C. R. Thomas, Characterising latex particles and fractal aggregates using image analysis, Colloid and Polymer Science 277 (1999) 325–333. URL: https://doi.org/10.1007/s003960050388. doi:10.1007/s003960050388.

[60] F. Martínez-Pedrero, M. Tirado-Miranda, A. Schmitt, F. Vereda, J. Callejas-Fernández, Structure and stability of aggregates formed by electrical double-layered magnetic particles, Colloids and Surfaces A: Physicochemical and Engineering Aspects 306 (2007) 158–165. URL: https://www.sciencedirect.com/science/article/pii/S0927775707002531. doi:https://doi.org/10.1016/j.colsurfa.2007.03.029, iNTERFACES AGAINST POLLUTION 2006.

[61] Q. Liao, L. Chen, X. Qu, X. Jin, Brownian dynamics simulation of film formation of mixed polymer latex in the water evaporation stage, Journal of Colloid and Interface Science 227 (2000) 84–94. URL: https://www.sciencedirect.com/science/article/pii/S002197970096867X. doi:https://doi.org/10.1006/jcis.2000.6867.

[62] L. Theodon, C. Coufort-Saudejaud, J. Debayle, Grape: A stochastic geometrical 3d model for aggregates of particles with tunable 2d morphological projected properties, Image Analysis & Stereology 42 (2023) 1–16. URL: https://www.ias-iss.org/ojs/IAS/article/view/2875. doi:10.5566/ias.2875.

[63] A. Spettl, S. Bachstein, M. Dosta, M. Goslinska, S. Heinrich, V. Schmidt, Bonded-particle extraction and stochastic modeling of internal agglomerate structures, Advanced Powder Technology 27 (2016) 1761–1774. URL: https://www.sciencedirect.com/science/article/pii/S092188311630142X. doi:https://doi.org/10.1016/j.apt.2016.06.007.

[64] R. Pashminehazar, A. Kharaghani, E. Tsotsas, Three dimensional characterization of morphology and internal structure of soft material agglomerates produced in spray fluidized bed by x-ray tomography, Powder Technology 300 (2016) 46–60. URL: https://www.sciencedirect.com/science/article/pii/S0032591016301565. doi:https://doi.org/10.1016/j.powtec.2016.03.053, 7th International Granulation Workshop 2015: Granulation across the length scales.

[65] R. Pashminehazar, S. J. Ahmed, A. Kharaghani, E. Tsotsas, Spatial morphology of maltodextrin agglomerates from x-ray microtomographic data: Real structure evaluation vs. spherical primary particle model, Powder Technology 331 (2018) 204–217. URL: https://www.sciencedirect.com/science/article/pii/S0032591018301918. doi:https://doi.org/10.1016/j.powtec.2018.03.008.

[66] I. Atalar, F. Yazici, Effect of different binders on reconstitution behaviors and physical, structural, and morphological properties of fluidized bed agglomerated yoghurt powder, Drying Technology 37 (2019) 1656–1664. URL: https://doi.org/10.1080/07373937.2018.1529038. doi:10.1080/07373937.2018.1529038. arXiv:https://doi.org/10.1080/07373937.2018.1529038.

[67] M. Manno, E. F. Craparo, A. Podestà, D. Bulone, R. Carrotta, V. Martorana, G. Tiana, P. L. San Biagio, Kinetics of different processes in human insulin amyloid formation, Journal of Molecular Biology 366 (2007) 258–274. URL: https://www.sciencedirect.com/science/article/pii/S0022283606015373. doi:https://doi.org/10.1016/j.jmb.2006.11.008.

[68] W. Hoyer, D. Cherny, V. Subramaniam, T. M. Jovin, Rapid self-assembly of α-synuclein observed by in situ atomic force microscopy, Journal of Molecular Biology 340 (2004) 127–139. URL: https://www.sciencedirect.com/science/article/pii/

S0022283604004991. doi:https://doi.org/10.1016/j.jmb.2004.04.051.

[69] M. M. Apetri, N. C. Maiti, M. G. Zagorski, P. R. Carey, V. E. Anderson, Secondary structure of α-synuclein oligomers: Characterization by raman and atomic force microscopy, Journal of Molecular Biology 355 (2006) 63–71. URL: https://www.sciencedirect.com/science/article/pii/S0022283605013318. doi:https://doi.org/10.1016/j.jmb.2005.10.071.

[70] W. B. Stine, S. W. Snyder, U. S. Ladror, W. S. Wade, M. F. Miller, T. J. Perun, T. F. Holzman, G. A. Krafft, The nanometer-scale structure of amyloid-β visualized by atomic force microscopy, Journal of Protein Chemistry 15 (1996) 193–203. URL: https://doi.org/10.1007/BF01887400. doi:10.1007/BF01887400.

[71] R. Liu, C. McAllister, Y. Lyubchenko, M. R. Sierks, Residues 17–20 and 30–35 of beta-amyloid play critical roles in aggregation, Journal of Neuroscience Research 75 (2004) 162–171. URL: https://onlinelibrary.wiley.com/doi/abs/10.1002/jnr.10859. doi:https://doi.org/10.1002/jnr.10859. arXiv:https://onlinelibrary.wiley.com/doi/pdf/10.1002/jnr.10859.

[72] R. Jansen, W. Dzwolak, R. Winter, Amyloidogenic self-assembly of insulin aggregates probed by high resolution atomic force microscopy, Biophysical Journal 88 (2005) 1344–1353. URL: https://www.sciencedirect.com/science/article/pii/S0006349505732008. doi:https://doi.org/10.1529/biophysj.104.048843.

[73] J. Adamcik, J.-M. Jung, J. Flakowski, P. De Los Rios, G. Dietler, R. Mezzenga, Understanding amyloid aggregation by statistical analysis of atomic force microscopy images, Nature Nanotechnology 5 (2010) 423–428. URL: https://doi.org/10.1038/nnano.2010.59. doi:10.1038/nnano.2010.59.

[74] S. Tanaka, Z. Kato, N. Uchida, K. Uematsu, Direct observation of aggregates and agglomerates in alumina granules, Powder Technology 129 (2003) 153–155. URL: https://www.sciencedirect.com/science/article/pii/S0032591002002267. doi:https://doi.org/10.1016/S0032-5910(02)00226-7.

[75] S. Tohno, K. Takahashi, Shape analysis of particles by an image scanner and a microcomputer: Application to agglomerated aerosol particles [translated]¡sup¿†¡/sup¿, KONA Powder and Particle Journal 6 (1988) 2–14. doi:10.14356/kona.1988004.

[76] B. Bernard-Michel, S. Rohani, M.-N. Pons, H. Vivier, H. S. Hundal, Classification of crystal shape using fourier descriptors and mathematical morphology, Particle & Particle Systems Characterization 14 (1997) 193–200. URL: https://onlinelibrary.wiley.com/doi/abs/10.1002/ppsc.199700041. doi:https://doi.org/10.1002/ppsc.199700041. arXiv:https://onlinelibrary.wiley.com/doi/pdf/10.1002/ppsc.199700041.

[77] M. Vučak, M. Pons, J. Perić, H. Vivier, Effect of precipitation conditions on the morphology of calcium carbonate: quantification of crystal shapes using image analysis, Powder Technology 97 (1998) 1–5. URL: https://www.sciencedirect.com/science/article/pii/S0032591097033755. doi:https://doi.org/10.1016/S0032-5910(97)03375-5.

[78] M.-N. Pons, H. Vivier, V. Delcour, J.-R. Authelin, L. Paillères-Hubert, Morphological analysis of pharmaceutical powders, Powder Technology 128 (2002) 276–286. URL: https://www.sciencedirect.com/science/article/pii/S0032591002001778. doi:https://doi.org/10.1016/S0032-5910(02)00177-8, 3rd French Colloquium on Powder Science & Technology.

[79] M. Pons, V. Plagnieux, H. Vivier, D. Audet, Comparison of methods for the characterisation by image analysis of crystalline agglomerates: The case of gibbsite, Powder Technology 157 (2005) 57–66. URL: https://www.sciencedirect.com/science/article/pii/S0032591005002263. doi:https://doi.org/10.1016/j.powtec.2005.05.011, 4th French Meeting on Powder Science and Technology.

[80] E. V. Ershov, V. V. Selivanovskikh, O. G. Ganicheva, Methods of handling of in-bulk agglomeration layer image representation for granulometric composition assessment, Pattern Recognition and Image Analysis 19 (2009) 103–105. URL: https://doi.org/10.1134/S1054661809010180. doi:10.1134/S1054661809010180.

[81] R. Fernandez Martinez, A. Okariz, J. Ibarretxe, M. Iturrondobeitia, T. Guraya, Use of decision tree models based on evolutionary algorithms for the morphological classification of reinforcing nano-particle aggregates, Computational Materials Science 92 (2014) 102–113. URL: https://www.sciencedirect.com/science/article/pii/S0927025614003565. doi:https://doi.org/10.1016/j.commatsci.2014.05.038.

[82] M. Frei, F. E. Kruis, Fully automated primary particle size analysis of agglomerates on transmission electron microscopy images via artificial neural networks, Powder Technology 332 (2018) 120–130. URL: https://www.sciencedirect.com/science/article/pii/S0032591018302249. doi:https://doi.org/10.1016/j.powtec.2018.03.032.

[83] M. Frei, F. Kruis, Image-based size analysis of agglomerated and partially sintered particles via convolutional neural networks, Powder Technology 360 (2020) 324–336. URL: https://www.sciencedirect.com/science/article/pii/S003259101930854X. doi:https://doi.org/10.1016/j.powtec.2019.10.020.

[84] P. Monchot, L. Coquelin, K. Guerroudj, N. Feltin, A. Delvallée, L. Crouzier, N. Fischer, Deep learning based instance segmentation of titanium dioxide particles in the form of agglomerates in scanning electron microscopy, Nanomaterials 11 (2021). URL: https://www.mdpi.com/2079-4991/11/4/968. doi:10.3390/nano11040968.

[85] B. Rühle, J. F. Krumrey, V.-D. Hodoroaba, Workflow towards automated segmentation of agglomerated, non-spherical particles from electron microscopy images using artificial neural networks, Scientific Reports 11 (2021) 4942. URL: https://doi.org/10.1038/s41598-021-84287-6. doi:10.1038/s41598-021-84287-6.

[86] N. Faria, M. Pons, S. Feyo de Azevedo, F. Rocha, H. Vivier, Quantification of the morphology of sucrose crystals by image analysis, Powder Technology 133 (2003) 54–67. URL: https://www.sciencedirect.com/science/article/pii/S0032591003000780. doi:https://doi.org/10.1016/S0032-5910(03)00078-0.

[87] C. Turchiuli, E. Castillo-Castaneda, Agglomerates structure characterization using 3d-image reconstruction, Particle & Particle Systems Characterization 26 (2009) 25–33. URL: https://onlinelibrary.wiley.com/doi/abs/10.1002/ppsc.200700028. doi:https://doi.org/10.1002/ppsc.200700028. arXiv:https://onlinelibrary.wiley.com/doi/pdf/10.1002/ppsc.2007

[88] G. Dacanal, T. Hirata, F. Menegalli, Fluid dynamics and morphological characterization of soy protein isolate particles obtained by agglomeration in pulsed-fluid bed, Powder Technology 247 (2013) 222–230. URL: https://www.sciencedirect.com/science/article/pii/S0032591013004609. doi:https://doi.org/10.1016/j.powtec.2013.07.001.

[89] F. Z. Vissotto, R. C. Giarola, L. C. Jorge, G. T. Makita, G. M. B. Q. Candido, M. I. Rodrigues, F. C. Menegalli, Morphological characterization with image analysis of cocoa beverage powder agglomerated with steam, Food Science and Technology 34 (2014). URL: https://doi.org/10.1590/1678-457X.6246. doi:10.1590/1678-457X.6246.

[90] J. L. Ortega-Vinuesa, P. Tengvall, I. Lundström, Aggregation of hsa, igg, and fibrinogen on methylated silicon surfaces, Journal of Colloid and Interface Science 207 (1998) 228–239. URL: https://www.sciencedirect.com/science/article/pii/S0021979798956247. doi:https://doi.org/10.1006/jcis.1998.5624.

[91] M. Lapuerta, J. Barba, A. D. Sediako, M. R. Kholghy, M. J. Thomson, Morphological analysis of soot agglomerates from biodiesel surrogates in a coflow burner, Journal of Aerosol Science 111 (2017) 65–74. URL: https://www.sciencedirect.com/science/article/pii/S0021850217301180. doi:https://doi.org/10.1016/j.jaerosci.2017.06.004.

[92] C. Kong, D. Yu, Q. Yao, S. Li, Morphological changes of nano-al agglomerates during reaction and its effect on combustion, Combustion and Flame 165 (2016) 11–20. URL: https://www.sciencedirect.com/science/article/pii/S0010218015003065. doi:https://doi.org/10.1016/j.combustflame.2015.09.003.

[93] O. Cohen, D. Michaels, Y. Yavor, Agglomeration in composite propellants containing different nano-aluminum powders, Propellants, Explosives, Pyrotechnics 47 (2022) e202100320. URL: https://onlinelibrary.wiley.com/doi/abs/10.1002/prep.202100320. doi:https://doi.org/10.1002/prep.202100320.

arXiv:https://onlinelibrary.wiley.com/doi/pdf/10.1002/prep.202100320.

[94] F. Maggi, A. Bandera, L. T. D. Luca, V. Thoorens, J. F. Trubert, T. L. Jackson, Agglomeration in solid rocket propellants: Novel experimental and modeling methods, 2011.

[95] B. Jin, Z. xin Wang, G. Xu, W. Ao, P. jin Liu, Three-dimensional spatial distributions of agglomerated particles on and near the burning surface of aluminized solid propellant using morphological digital in-line holography, Aerospace Science and Technology 106 (2020) 106066. URL: https://www.sciencedirect.com/science/article/pii/S1270963820307483. doi:https://doi.org/10.1016/j.ast.2020.106066.

[96] P. M. Jenneson, O. Gundogdu, In situ x-ray imaging of nanoparticle agglomeration in fluidized beds, Applied Physics Letters 88 (2006). URL: https://doi.org/10.1063/1.2166486. doi:10.1063/1.2166486. arXiv:https://pubs.aip.org/aip/apl/article-pdf/doi/10.1063/1.2166486/13111981/034103_1_online.pdf. 034103.

[97] B. Sung, L. Abelmann, Agglomeration structure of superparamagnetic nanoparticles in a nematic liquid crystal medium: Image analysis datasets based on cryo-electron microscopy and polarised optical microscopy techniques, Data in Brief 34 (2021) 106716. URL: https://www.sciencedirect.com/science/article/pii/S2352340921000020. doi:https://doi.org/10.1016/j.dib.2021.106716.

[98] A. J. Cecil, J. E. Payne, L. T. Hawtrey, B. King, G. A. Willing, S. J. Williams, Nonlinear agglomeration of bimodal colloids under microgravity, Gravitational and Space Research 10 (2022) 1–9. URL: https://doi.org/10.2478/gsr-2022-0001. doi:doi:10.2478/gsr-2022-0001.

[99] C. Neef, C. Jähne, H.-P. Meyer, R. Klingeler, Morphology and agglomeration control of limnpo4 micro- and nanocrystals, Langmuir 29 (2013) 8054–8060. URL: https://doi.org/10.1021/la3046498. doi:10.1021/la3046498.

[100] T.-H. Kim, J.-Y. Yi, C.-Y. Jung, E. Jeong, S.-C. Yi, Solvent effect on the nafion agglomerate morphology in the catalyst layer of the proton exchange membrane fuel cells, International Journal of Hydrogen Energy 42 (2017) 478–485. URL: https://www.sciencedirect.com/science/article/pii/S0360319916335571. doi:https://doi.org/10.1016/j.ijhydene.2016.12.015.

[101] F. C. Cetinbas, R. K. Ahluwalia, N. N. Kariuki, V. D. Andrade, D. J. Myers, Effects of porous carbon morphology, agglomerate structure and relative humidity on local oxygen transport resistance, Journal of The Electrochemical Society 167 (2019) 013508. URL: https://dx.doi.org/10.1149/2.0082001JES. doi:10.1149/2.0082001JES.

[102] W. G. Shin, J. Wang, M. Mertler, B. Sachweh, H. Fissan, D. Y. Pui, The effect of particle morphology on unipolar diffusion charging of nanoparticle agglomerates in the transition regime, Journal of Aerosol Science 41 (2010) 975–986. URL: https://www.sciencedirect.com/science/article/pii/S0021850210001539. doi:https://doi.org/10.1016/j.jaerosci.2010.07.004.

[103] P.-J. De Temmerman, E. Van Doren, E. Verleysen, Y. Van der Stede, M. A. D. Francisco, J. Mast, Quantitative characterization of agglomerates and aggregates of pyrogenic and precipitated amorphous silica nanomaterials by transmission electron microscopy, Journal of Nanobiotechnology 10 (2012) 24. URL: https://doi.org/10.1186/1477-3155-10-24. doi:10.1186/1477-3155-10-24.

[104] C. Bower, C. Washington, T. Purewal, The use of image analysis to characterize aggregates in a shear field, Colloids and Surfaces A: Physicochemical and Engineering Aspects 127 (1997) 105–112. URL: https://www.sciencedirect.com/science/article/pii/S0927775796039453. doi:https://doi.org/10.1016/S0927-7757(96)03945-3.

[105] J. J. Reyes-Salgado, Study of complex morphology of agglomerations formed by graphite nanoinclusions and its effect on the mechanical properties of the composite materials, Journal of Physics D: Applied Physics 51 (2018) 295301. URL: https://dx.doi.org/10.1088/1361-6463/aacaa6. doi:10.1088/1361-6463/aacaa6.

[106] F. Einar Kruis, J. van Denderen, H. Buurman, B. Scarlett, Characterization of agglomerated and aggregated aerosol particles using image analysis, Particle & Particle Systems Characterization 11 (1994) 426–435. URL: https://onlinelibrary.wiley.com/doi/abs/10.1002/ppsc.19940110605. doi:https://doi.org/10.1002/ppsc.19940110605. arXiv:https://onlinelibrary.wiley.com/doi/pdf/10.1002/ppsc.1994

[107] S. Weinbruch, P. van Aken, M. Ebert, Y. Thomassen, A. Skogstad, V. P. Chashchin, A. Nikonov, The heterogeneous composition of working place aerosols in a nickel refinery: a transmission and scanning electron microscope study, J. Environ. Monit. 4 (2002) 344–350. URL: http://dx.doi.org/10.1039/B110504N. doi:10.1039/B110504N.

[108] J. McCallister, M. Gammage, J. Keto, M. Becker, D. Kovar, Influence of agglomerate morphology on micro cold spray of ag nanopowders, Journal of Aerosol Science 151 (2021) 105648. URL: https://www.sciencedirect.com/science/article/pii/S002185022030135X. doi:https://doi.org/10.1016/j.jaerosci.2020.105648.

[109] P. Born, T. Kraus, Ligand-dominated temperature dependence of agglomeration and morphology in alkyl-thiol-coated gold nanoparticles, Phys. Rev. E 87 (2013) 062313. URL: https://link.aps.org/doi/10.1103/PhysRevE.87.062313. doi:10.1103/PhysRevE.87.062313.

[110] T. W. Vasicek, S. V. Jenkins, L. Vaz, J. Chen, J. A. Stenken, Thermoresponsive nanoparticle agglomeration/aggregation in salt solutions: Dependence on graft density, Journal of Colloid and Interface Science 506 (2017) 338–345. URL: https://www.sciencedirect.com/science/article/pii/S0021979717308123. doi:https://doi.org/10.1016/j.jcis.2017.07.044.

[111] C. Y. Tai, P.-C. Chen, Nucleation, agglomeration and crystal morphology of calcium carbonate, AIChE Journal 41 (1995) 68–77. URL: https://aiche.onlinelibrary.wiley.com/doi/abs/10.1002/aic.690410108. doi:https://doi.org/10.1002/aic.690410108. arXiv:https://aiche.onlinelibrary.wiley.com/doi/pdf/10.1002/aic

[112] C. Frances, N. Le Bolay, K. Belaroui, M. Pons, Particle morphology of ground gibbsite in different grinding environments, International Journal of Mineral Processing 61 (2001) 41–56. URL: https://www.sciencedirect.com/science/article/pii/S0301751600000259. doi:https://doi.org/10.1016/S0301-7516(00)00025-9.

[113] J. Lins, T. Harweg, F. Weichert, K. Wohlgemuth, Potential of deep learning methods for deep level particle characterization in crystallization, Applied Sciences 12 (2022). URL: https://www.mdpi.com/2076-3417/12/5/2465. doi:10.3390/app12052465.

[114] N. Otsu, A threshold selection method from gray-level histograms, IEEE Transactions on Systems, Man, and Cybernetics 9 (1979) 62–66. doi:10.1109/TSMC.1979.4310076.

[115] M. Sezgin, B. Sankur, Survey over image thresholding techniques and quantitative performance evaluation, Journal of Electronic Imaging 13 (2004) 146 – 165. URL: https://doi.org/10.1117/1.1631315. doi:10.1117/1.1631315.

[116] J. Bals, M. Epple, Deep learning for automated size and shape analysis of nanoparticles in scanning electron microscopy, RSC Adv. 13 (2023) 2795–2802. URL: http://dx.doi.org/10.1039/D2RA07812K. doi:10.1039/D2RA07812K.

[117] M. Ester, H.-P. Kriegel, J. Sander, X. Xu, A density-based algorithm for discovering clusters in large spatial databases with noise, in: Proceedings of the Second International Conference on Knowledge Discovery and Data Mining, KDD'96, AAAI Press, 1996, p. 226–231.

[118] Y. Huo, T. Liu, X. Z. Wang, C. Y. Ma, X. Ni, Online detection of particle agglomeration during solution crystallization by microscopic double-view image analysis, Industrial & Engineering Chemistry Research 56 (2017) 11257–11269. URL: https://doi.org/10.1021/acs.iecr.7b02439. doi:10.1021/acs.iecr.7b02439.

[119] F. Ros, S. Guillaume, F. Sevila, Agglomerates processing on in-flight images of granular products, in: S. S. Breidenthal, A. A. Desrochers (Eds.), Vision, Sensors, and Control for Automated Manufacturing Systems, volume 2063, International Society for Optics and Photonics, SPIE, 1993, pp. 120 – 128. URL: https://doi.org/10.1117/12.164960. doi:10.1117/12.164960.

[120] D. R. Ochsenbein, T. Vetter, S. Schorsch, M. Morari, M. Mazzotti, Agglomeration of needle-like crystals in suspension: I. measurements, Crystal Growth & Design 15 (2015) 1923–1933. doi:10.1021/acs.cgd.5b00094.

[121] Y. Huo, T. Liu, H. Liu, C. Y. Ma, X. Z. Wang, In-situ crystal morphology identification using imaging analysis with application to the l-glutamic acid crystallization, Chemical Engineering Science 148 (2016) 126–139. URL: https://www.sciencedirect.com/science/article/pii/S000925091630152X. doi:https://doi.org/10.1016/j.ces.2016.03.039.

[122] J. López-de Uralde, I. Ruiz, I. Santos, A. Zubillaga, P. G. Bringas, A. Okariz, T. Guraya, Automatic morphological categorisation of carbon black nano-aggregates, in: P. G. Bringas, A. Hameurlain, G. Quirchmayr (Eds.), Database and Expert Systems Applications, Springer Berlin Heidelberg, Berlin, Heidelberg, 2010, pp. 185–193.

[123] C. Lee, T. A. Kramer, Prediction of three-dimensional fractal dimensions using the two-dimensional properties of fractal aggregates, Advances in Colloid and Interface Science 112 (2004) 49–57. URL: https://www.sciencedirect.com/science/article/pii/S0001868604000454. doi:https://doi.org/10.1016/j.cis.2004.07.001.

[124] J. S. Philo, A critical review of methods for size characterization of non-particulate protein aggregates, Curr Pharm Biotechnol 10 (2009) 359–372.

[125] C. M. Sorensen, The mobility of fractal aggregates: A review, Aerosol Science and Technology 45 (2011) 765–779. URL: https://doi.org/10.1080/02786826.2011.560909. doi:10.1080/02786826.2011.560909. arXiv:https://doi.org/10.1080/02786826.2011.560909.

[126] J. J. Komba, J. K. Anochie-Boateng, W. van der Merwe Steyn, Analytical and laser scanning techniques to determine shape properties of aggregates, Transportation Research Record 2335 (2013) 60–71. URL: https://doi.org/10.3141/2335-07. doi:10.3141/2335-07. arXiv:https://doi.org/10.3141/2335-07.

[127] S. Amin, G. V. Barnett, J. A. Pathak, C. J. Roberts, P. S. Sarangapani, Protein aggregation, particle formation, characterization & rheology, Current Opinion in Colloid & Interface Science 19 (2014) 438–449. URL: https://www.sciencedirect.com/science/article/pii/S135902941400096X. doi:https://doi.org/10.1016/j.cocis.2014.10.002.

[128] R. I. Jeldres, P. D. Fawell, B. J. Florio, Population balance modelling to describe the particle aggregation process: A review, Powder Technology 326 (2018) 190–207. URL: https://www.sciencedirect.com/science/article/pii/S003259101730983X. doi:https://doi.org/10.1016/j.powtec.2017.12.033.

[129] F. S. Ruggeri, T. Šneideris, M. Vendruscolo, T. P. Knowles, Atomic force microscopy for single molecule characterisation of protein aggregation, Archives of Biochemistry and Biophysics 664 (2019) 134–148. URL: https://www.sciencedirect.com/science/article/pii/S0003986118309330. doi:https://doi.org/10.1016/j.abb.2019.02.001.

[130] S. Zhang, R. Li, J. Pei, Evaluation methods and indexes of morphological characteristics of coarse aggregates for road materials: A comprehensive review, Journal of Traffic and Transportation Engineering (English Edition) 6 (2019) 256–272. URL: https://www.sciencedirect.com/science/article/pii/S2095756419301382. doi:https://doi.org/10.1016/j.jtte.2019.01.003.

[131] P. Thaker, N. Arora, Measurement of aggregate size and shape using image analysis, in: K. Dasgupta, A. S. Sajith, G. Unni Kartha, A. Joseph, P. E. Kavitha, K. Praseeda (Eds.), Proceedings of SECON'19, Springer International Publishing, Cham, 2020, pp. 739–747.

[132] V. Lotito, T. Zambelli, Pattern detection in colloidal assembly: A mosaic of analysis techniques, Advances in Colloid and Interface Science 284 (2020) 102252. URL: https://www.sciencedirect.com/science/article/pii/S0001868620302852. doi:https://doi.org/10.1016/j.cis.2020.102252.

[133] T. Watanabe-Nakayama, B. R. Sahoo, A. Ramamoorthy, K. Ono, High-speed atomic force microscopy reveals the structural dynamics of the amyloid-b and amylin aggregation pathways, International Journal of Molecular Sciences 21 (2020). URL: https://www.mdpi.com/1422-0067/21/12/4287. doi:10.3390/ijms21124287.

[134] F. Gong, Y. Liu, Z. You, X. Zhou, Characterization and evaluation of morphological features for aggregate in asphalt mixture: A review, Construction and Building Materials 273 (2021) 121989. URL: https://www.sciencedirect.com/science/article/pii/S0950061820339933. doi:https://doi.org/10.1016/j.conbuildmat.2020.121989.

[135] S. Matsutani, Y. Shimosako, Measuring agglomeration of agglomerated particles pictures, 2013. arXiv:1302.5150.

[136] M. Petrere, The variance of the index (r) of aggregation of clark and evans, Oecologia 68 (1985) 158–159. URL: https://doi.org/10.1007/BF00379489. doi:10.1007/BF00379489.

[137] A. K. Singh, E. Tsotsas, Stochastic model to simulate spray fluidized bed agglomeration: a morphological approach, Powder Technology 355 (2019) 449–460. URL: https://www.sciencedirect.com/science/article/pii/S0032591019305674. doi:https://doi.org/10.1016/j.powtec.2019.07.075.

[138] A.-F. Blandin, A. Rivoire, D. Mangin, J.-P. Klein, J.-M. Bossoutrot, Using in situ image analysis to study the kinetics of agglomeration in suspension, Particle & Particle Systems Characterization 17 (2000) 16–20. doi:https://doi.org/10.1002/(SICI)1521-4117(200003)17:1<16::AID-PPSC16>3.0.CO;2-I.

[139] S. R. Machinski, K. A. Richardson, A. Dogariu, An image analysis technique for assessing particle size and agglomeration tendency of slurries, MRS Online Proceedings Library 613 (2000) 611. URL: https://doi.org/10.1557/PROC-613-E6.1.1. doi:10.1557/PROC-613-E6.1.1.

[140] M. da Motta, M. N. Pons, N. Roche, Automated monitoring of activated sludge in a pilot plant using image analysis, Water Sci Technol 43 (2001) 91–96.

[141] A. Blandin, D. Mangin, A. Rivoire, J. Klein, J. Bossoutrot, Agglomeration in suspension of salicylic acid fine particles: influence of some process parameters on kinetics and agglomerate final size, Powder Technology 130 (2003) 316–323. URL: https://www.sciencedirect.com/science/article/pii/S0032591002002103. doi:https://doi.org/10.1016/S0032-5910(02)00210-3.

[142] A. Blandin, D. Mangin, C. Subero-Couroyer, A. Rivoire, J. Klein, J. Bossoutrot, Modelling of agglomeration in suspension: Application to salicylic acid microparticles, Powder Technology 156 (2005) 19–33. URL: https://www.sciencedirect.com/science/article/pii/S0032591005002792. doi:https://doi.org/10.1016/j.powtec.2005.05.049.

[143] C. Subero-Couroyer, D. Mangin, A. Rivoire, A. Blandin, J. Klein, Agglomeration in suspension of salicylic acid fine particles: Analysis of the wetting period and effect of the binder injection mode on the final agglomerate size, Powder Technology 161 (2006) 98–109. URL: https://www.sciencedirect.com/science/article/pii/S0032591005003815. doi:https://doi.org/10.1016/j.powtec.2005.08.014.

[144] J.-Q. Huang, Q. Zhang, G.-H. Xu, W.-Z. Qian, F. Wei, Substrate morphology induced self-organization into carbon nanotube arrays, ropes, and agglomerates, Nanotechnology 19 (2008) 435602. URL: https://dx.doi.org/10.1088/0957-4484/19/43/435602. doi:10.1088/0957-4484/19/43/435602.

[145] W. Li, A. Woldu, R. Kelly, J. McCool, R. Bruce, H. Rasmussen, J. Cunningham, D. Winstead, Measurement of drug agglomerates in powder blending simulation samples by near infrared chemical imaging, International Journal of Pharmaceutics 350 (2008) 369–373. URL: https://www.sciencedirect.com/science/article/pii/S0378517307007430. doi:https://doi.org/10.1016/j.ijpharm.2007.08.055.

[146] X. S. Shen, G. Z. Wang, X. Hong, W. Zhu, Nanospheres of silver nanoparticles: agglomeration, surface morphology control and application as sers substrates, Phys. Chem. Chem. Phys. 11 (2009) 7450–7454. URL: http://dx.doi.org/10.1039/B904712C. doi:10.1039/B904712C.

[147] K. Menzer, B. Krause, R. Boldt, B. Kretzschmar, R. Weidisch, P. Pötschke, Percolation behaviour of multiwalled carbon nanotubes of altered length and primary agglomerate morphology in melt mixed isotactic polypropylene-based composites, Composites Science and Technology 71 (2011) 1936–1943. URL: https://www.sciencedirect.com/science/article/pii/S0266353811003368. doi:https://doi.org/10.1016/j.compscitech.2011.09.009.

[148] K. Ono, M. Yanaka, S. Tanaka, Y. Saito, H. Aoki, O. Fukuda, T. Aoki, T. Yamaguchi, Influence of furnace temperature and residence

time on configurations of carbon black, Chemical Engineering Journal 200-202 (2012) 541–548. URL: https://www.sciencedirect.com/science/article/pii/S1385894712007826. doi:https://doi.org/10.1016/j.cej.2012.06.061.

[149] X. Cai, B. Li, Y. Pan, G. Wu, Morphology evolution of immiscible polymer blends as directed by nanoparticle self-agglomeration, Polymer 53 (2012) 259–266. URL: https://www.sciencedirect.com/science/article/pii/S0032386111009566. doi:https://doi.org/10.1016/j.polymer.2011.11.032.

[150] M. Dadkhah, M. Peglow, E. Tsotsas, Characterization of the internal morphology of agglomerates produced in a spray fluidized bed by x-ray tomography, Powder Technology 228 (2012) 349–358. URL: https://www.sciencedirect.com/science/article/pii/S0032591012003786. doi:https://doi.org/10.1016/j.powtec.2012.05.051.

[151] K. Ono, M. Yanaka, Y. Saito, H. Aoki, O. Fukuda, T. Aoki, T. Yamaguchi, Effect of benzene–acetylene compositions on carbon black configurations produced by benzene pyrolysis, Chemical Engineering Journal 215-216 (2013) 128–135. URL: https://www.sciencedirect.com/science/article/pii/S1385894712014568. doi:https://doi.org/10.1016/j.cej.2012.10.085.

[152] K. Høydalsvik, J. Bø Fløystad, T. Zhao, M. Esmaeili, A. Diaz, J. W. Andreasen, R. H. Mathiesen, M. Rønning, D. W. Breiby, In situ X-ray ptychography imaging of high-temperature CO_2 acceptor particle agglomerates, Applied Physics Letters 104 (2014) 241909. doi:10.1063/1.4884598.

[153] M. Dadkhah, E. Tsotsas, Study of the morphology of solidified binder in spray fluidized bed agglomerates by x-ray tomography, Powder Technology 264 (2014) 256–264. URL: https://www.sciencedirect.com/science/article/pii/S0032591014004926. doi:https://doi.org/10.1016/j.powtec.2014.05.037.

[154] B. Yang, S. Song, A. Lopez-Valdivieso, Morphology of hydrophobic agglomerates of molybdenite fines in aqueous suspensions, Separation Science and Technology 50 (2015) 1560–1564. URL: https://doi.org/10.1080/01496395.2014.975365. doi:10.1080/01496395.2014.975365. arXiv:https://doi.org/10.1080/01496395.2014.975365.

[155] Y. Bai, L. Yan, J. Wang, Z. Yin, N. Chen, F. Wang, Z. Tan, Tailoring film agglomeration for preparation of silver nanoparticles with controlled morphology, Materials & Design 103 (2016) 315–320. URL: https://www.sciencedirect.com/science/article/pii/S0264127516305640. doi:https://doi.org/10.1016/j.matdes.2016.04.081.

[156] S. J. Chen, C. Y. Qiu, A. H. Korayem, M. R. Barati, W. H. Duan, Agglomeration process of surfactant-dispersed carbon nanotubes in unstable dispersion: A two-stage agglomeration model and experimental evidence, Powder Technology 301 (2016) 412–420. URL: https://www.sciencedirect.com/science/article/pii/S0032591016303722. doi:https://doi.org/10.1016/j.powtec.2016.06.033.

[157] Z. Yang, X. Chen, Z. Xu, M. Xiao, L. Hong, T. Ngai, Shear-assisted fabrication of block copolymer agglomerates with various morphologies in viscous medium, Langmuir 33 (2017) 2829–2836. URL: https://doi.org/10.1021/acs.langmuir.7b00119. doi:10.1021/acs.langmuir.7b00119.

[158] Z. Dong, Z. Liu, P. Wang, X. Gong, Nanostructure characterization of asphalt-aggregate interface through molecular dynamics simulation and atomic force microscopy, Fuel 189 (2017) 155–163. URL: https://www.sciencedirect.com/science/article/pii/S0016236116310390. doi:https://doi.org/10.1016/j.fuel.2016.10.077.

[159] K. Zou, T. Liu, Y. Huo, F. Zhang, X. Ni, Image analysis for in-situ detection of agglomeration for needle-like crystals, in: 2017 36th Chinese Control Conference (CCC), 2017, pp. 11515–11520. doi:10.23919/ChiCC.2017.8029197.

[160] D. Bartczak, J. Davies, C. Gollwitzer, M. Krumrey, H. Goenaga-Infante, Changes in silica nanoparticles upon internalisation by cells: size, aggregation/agglomeration state, mass- and number-based concentrations, Toxicol. Res. 7 (2018) 172–181. URL: http://dx.doi.org/10.1039/C7TX00323D. doi:10.1039/C7TX00323D.

[161] U. M. Engelmann, E. M. Buhl, S. Draack, T. Viereck, F. Ludwig, T. Schmitz-Rode, I. Slabu, Magnetic relaxation of agglomerated and immobilized iron oxide nanoparticles for hyperthermia and imaging applications, IEEE Magnetics Letters 9 (2018) 1–5. doi:10.1109/LMAG.2018.2879034.

[162] G. Zhang, L. Zhang, J. Wang, Z. Chi, E. Hu, A new multiple-time-step three-dimensional discrete element modeling of aerosol acoustic agglomeration, Powder Technology 323 (2018) 393–402. URL: https://www.sciencedirect.com/science/article/pii/S003259101730832X. doi:https://doi.org/10.1016/j.powtec.2017.10.036.

[163] M. I. A. Barustan, S.-M. Jung, Morphology of iron and agglomeration behaviour during reduction of iron oxide fines, Metals and Materials International 25 (2019) 1083–1097. URL: https://doi.org/10.1007/s12540-019-00259-6. doi:10.1007/s12540-019-00259-6.

[164] L. Le Barbenchon, J. Girardot, J.-B. Kopp, P. Viot, Multi-scale foam : 3d structure/compressive behaviour relationship of agglomerated cork, Materialia 5 (2019) 100219. URL: https://www.sciencedirect.com/science/article/pii/S2589152919300146. doi:https://doi.org/10.1016/j.mtla.2019.100219.

[165] J. Weston, J. Chun, G. Schenter, K. Weigandt, M. Zong, X. Zhang, K. Rosso, L. Anovitz, Connecting particle interactions to agglomerate morphology and rheology of boehmite nanocrystal suspensions, Journal of Colloid and Interface Science 572 (2020) 328–339. URL: https://www.sciencedirect.com/science/article/pii/S0021979720304100. doi:https://doi.org/10.1016/j.jcis.2020.03.109.

[166] Z. M. Lu, L. Zhang, D. M. Fan, N. M. Yao, C. X. Zhang, Crystal texture recognition system based on image analysis for the analysis of agglomerates, Chemometrics and Intelligent Laboratory Systems 200 (2020) 103985. URL: https://www.sciencedirect.com/science/article/pii/S0169743919307695. doi:https://doi.org/10.1016/j.chemolab.2020.103985.

[167] E. Zhalehrajabi, K. K. Lau, K. KuShaari, W. H. Tay, T. Hagemeier, A. Idris, Modelling of urea aggregation efficiency via particle tracking velocimetry in fluidized bed granulation, Chemical Engineering Science 223 (2020) 115737. URL: https://www.sciencedirect.com/science/article/pii/S0009250920302694. doi:https://doi.org/10.1016/j.ces.2020.115737.

[168] S. Wang, H. Liu, C. Yang, Y. Li, Experimental investigation on the microstructure of fluidized nanoparticle agglomerates by tem image analysis, The Canadian Journal of Chemical Engineering 99 (2021) 1125–1136. URL: https://onlinelibrary.wiley.com/doi/abs/10.1002/cjce.23908. doi:https://doi.org/10.1002/cjce.23908. arXiv:https://onlinelibrary.wiley.com/doi/pdf/10.1002/cjce.2390

[169] A. Lowe, G. Singh, H.-K. Chan, A. Masri, S. Cheng, A. Kourmatzis, Fragmentation dynamics of single agglomerate-to-wall impaction, Powder Technology 378 (2021) 561–575. URL: https://www.sciencedirect.com/science/article/pii/S0032591020309645. doi:https://doi.org/10.1016/j.powtec.2020.10.021.

[170] P. Romphophak, C. Coufort-Saudejaud, C. Le Men, P. Painmanakul, A. Liné, Analysis of flocculation in a jet clarifier. part 2 - analysis of aggregate size distribution versus camp number, Chemical Engineering Research and Design 175 (2021) 392–402. URL: https://www.sciencedirect.com/science/article/pii/S0263876221003683. doi:https://doi.org/10.1016/j.cherd.2021.09.008.

[171] Z. Shen, Q. Zhang, Hydrophobic agglomeration behavior of rhodochrosite fines co-induced by oleic acid and shearing, Separation and Purification Technology 282 (2022) 120115. URL: https://www.sciencedirect.com/science/article/pii/S1383586621018207. doi:https://doi.org/10.1016/j.seppur.2021.120115.

[172] H. Müller, L. Barthel, S. Schmideder, T. Schütze, V. Meyer, H. Briesen, From spores to fungal pellets: A new high-throughput image analysis highlights the structural development of aspergillus niger, Biotechnology and Bioengineering 119 (2022) 2182–2195. URL: https://onlinelibrary.wiley.com/doi/abs/10.1002/bit.28124. doi:https://doi.org/10.1002/bit.28124. arXiv:https://onlinelibrary.wiley.com/doi/pdf/10.1002/bit.28124

[173] R. Zhang, Z. Yang, R. Detwiler, D. Li, G. Ma, R. Hu,

Y.-F. Chen, Liquid cohesion induced particle agglomeration enhances clogging in rock fractures, Geophysical Research Letters 50 (2023) e2022GL102097. URL: https://agupubs.onlinelibrary.wiley.com/doi/abs/10.1029/2022GL102097. doi:https://doi.org/10.1029/2022GL102097. arXiv:https://agupubs.onlinelibrary.wiley.com/doi/pdf/10.1029/2022GL102097, e2022GL102097 2022GL102097.